Contract No:

This document was prepared in conjunction with work accomplished under Contract No. DE-AC09-08SR22470 with the U.S. Department of Energy (DOE) Office of Environmental Management (EM).

Disclaimer:

Impact of Permanganate Oxidation of Glycolate on Corrosion of the Defense Waste Processing Facility (DWPF) Recycle Collection Tank (RCT), Transfer-line and Waste Tank Materials of Construction (MoC)

Roderick E. Fuentes

January 2020

SRNL-STI-2019-00742, Revision 0

DISCLAIMER

Printed in the United States of America

Prepared for
U.S. Department of Energy

SRNL-STI-2019-00742
Revision 0

Keywords: *Defense Waste Processing Facility, Recycle Collection Tank, Transfer-line, Tank Farm, Glycolate Destruction, Permanganate, Corrosion*

Retention: *Permanent*

Impact of Permanganate Oxidation of Glycolate on Corrosion of the Defense Waste Processing Facility (DWPF) Recycle Collection Tank (RCT), Transfer-line and Waste Tank Materials of Construction (MoC)

R. E. Fuentes

January 2020

Prepared for the U.S. Department of Energy under contract number DE-AC09-08SR22470.

Savannah River National Laboratory™
OPERATED BY SAVANNAH RIVER NUCLEAR SOLUTIONS

REVIEWS AND APPROVALS

AUTHORS:

R. E. Fuentes, Materials Science and Engineering Date

TECHNICAL REVIEW:

J. I. Mickalonis, Materials Science and Engineering, Reviewed per E7 2.60 Date

APPROVAL:

B. J. Wiersma, Manager Date
Materials Science and Engineering

S. D. Fink, Director
Chemical Processing Technologies Date

T. H. Huff, Manager Date
DWPF/Saltstone Engineering

J. E. Occhipinti, Manager Date
Tank Farm Engineering

ACKNOWLEDGEMENTS

The author wants to acknowledge the technical assistance provided by Tracy Murphy. Thanks to Jack Zamecnik and Matthew Siegfried for providing simulant information including chemical analysis and for facilitating the transfer of Sludge Receipt and Adjustment Tank (SRAT) component and permanganate in solution. Thanks also to Thomas Peters and Charles Nash for letting me borrow laboratory equipment to conduct some experiments. Also, many thanks to Bruce Wiersma and John Mickalonis for providing consultation and background information for the design of experiments and analysis. I would also like to acknowledge the help provided by William Ramsey and Bill Holtzscheiter for supporting the testing and providing input.

EXECUTIVE SUMMARY

Savannah River Remediation (SRR) is evaluating the use of glycolic acid to replace formic acid as an alternate reductant for the Defense Waste Processing Facility (DWPF) at Savannah River Site (SRS). The replacement is aimed at reducing facility hazards, improving pH stability and rheological control, and lowering off gas production. Glycolate, which is the product that may remain, can also be carried downstream to High-Level Waste and Low-Level Waste facilities. Complete oxidation of glycolate and other organic species from the Sludge Receipt and Adjustment Tank (SRAT) may be necessary to minimize thermolytic hydrogen generation that can cause flammability issues.

The glycolate oxidation may be performed in the Recycle Collection Tank (RCT). The RCT heel would be adjusted with sodium hydroxide to maintain the solution caustic and sodium nitrite as corrosion inhibitor prior to the addition of condensate that can be from the contents of the Slurry Mix Evaporator Condensate Tank (SMECT) or Offgas Condensate Tank (OGCT). The RCT tank collects the waste to be transferred via the Low Point Pump Pit – Recycle Pump Tank (LPPP-RPT) through a jacketed transfer-line to the Tank Farm facility. Scoping studies were performed to evaluate an oxidizing agent and sodium permanganate was selected as the best option for glycolate destruction. Testing was recommended to determine the impact on the Materials of Construction (MoC) due to the addition of sodium permanganate. The targeted concentration of sodium permanganate used equated to a 7:1 molar permanganate to glycolate ratio (nominally 0.002 M permanganate). However, to conservatively maximize the permanganate corrosivity, in some cases no glycolate was added.

The results of this corrosion study using RCT simulants with maximum permanganate (no glycolate) and with SRAT component (includes glycolate) tested at different times after adding sodium permanganate (immediately and after more than three hours) showed that accelerated corrosion is not expected for MoCs of the RCT, transfer line, LPPP-RPT, the Tank Farm waste tanks (e.g., Tank 22) and the evaporator systems. The corrosion rates were within DWPF and Tank Farm norms of less than 1 mils per year (mpy).

Electrochemical corrosion methods, including Linear Polarization Resistance (LPR) and Cyclic Potentiodynamic Polarization (CPP), were successful in determining the instantaneous corrosion rate when the activity of the permanganate oxidation reaction was low (after three hours of addition and room temperature). The calculated instantaneous corrosion rate (obtained from LPR) was 0.38 mpy for A537 and 0.29 mpy for 304L and were comparable to corrosion rates obtained after coupon immersion for 1 week (0.39 mpy on average) at similar conditions. LPR tests using simulant with SRAT component added showed lower current densities than RCT simulant with maximum permanganate (without SRAT component) due to the decrease in permanganate oxidation activity since glycolate in the solution reacts with some of the permanganate.

Since some tests were performed when permanganate addition was most active (i.e., during the first three hours of addition for C-276 and platinum), the electrochemical activity of the permanganate was a contributing factor for the current density measured by LPR. The appearance of a layer on the surface also confirms the permanganate activity and, when removed, the surface was pristine with no localized corrosion. The high oxidation activity of permanganate was verified using a platinum electrode tested when permanganate was immediately added, since platinum is thermodynamically unfavorable for corrosion and not susceptible for localized corrosion.

The mass loss corrosion rates for A537 carbon steel flat coupon and stressed samples was 0.18 mpy and 0.08 mpy on average, respectively, after coupon immersion for four weeks with no indications of localized corrosion. A multicolored layer was observed on all the immersed coupons due to the permanganate oxidation exposure and was easily removed by immersing the coupons in 1 M HCl solution.

TABLE OF CONTENTS

LIST OF TABLES

LIST OF FIGURES

LIST OF ABBREVIATIONS

ACTL	Aiken County Technology Laboratory
ASTM	American Society for Testing and Materials
CPC	Chemical Process Cell
CPP	Cyclic Potentiodynamic Polarization
CV	Cyclic Voltammetry
DWPF	Defense Waste Processing Facility
HER	Hydrogen Evolution Reaction
LCM	Laser Confocal Microscope
LPPP-RPT	Low Point Pump Pit – Recycle Pump Tank
LPR	Linear Polarization Resistance
MoC	Materials of Construction
mpy	mils per year
OCP	Open Circuit Potential
OGCT	Offgas Condensate Tank
PTFE	Polytetrafluoroethylene
RCT	Recycle Collection Tank
SCC	Stress Corrosion Cracking
SCE	Saturated Calomel Electrode
SMECT	Slurry Mix Evaporator Condensate Tank
SRAT	Sludge Receipt and Adjustment Tank
SRNL	Savannah River National Laboratory
SRR	Savannah River Remediation
SRS	Savannah River Site
TTQAP	Task Technical and Quality Assurance Plan
TTR	Technical Task Request
WAC	Waste Acceptance Criteria
XRD	X-Ray Diffraction

1.0 Introduction

Glycolic acid is being evaluated by Savannah River Remediation (SRR) as an alternate reductant for the Defense Waste Processing Facility (DWPF) to replace formic acid [1]. The replacement is aimed at reducing facility hazards, improving pH stability and rheological control, and lowering off gas production. It will also reduce maintenance of laboratory equipment used in sample analysis. Laboratory studies performed at Savannah River National Laboratory (SRNL) indicated that the replacement to glycolic acid allows the reduction and removal of mercury in the Sludge Receipt and Adjustment Tank (SRAT) without significant hydrogen generation [2]. Due to the many advantages that glycolic acid can have over formic acid, testing was performed to evaluate the materials that can be in direct contact and the associated corrosion mechanisms compared with exposure to formic acid [3]. Glycolate, which is the product that may remain after using glycolic acid, can also be carried downstream to High-Level Waste and Low-Level Waste facilities. Testing has been done to perform a corrosion assessment for the components of the DWPF facility and other waste facilities that would be exposed to glycolic acid/glycolate [3],[4].

Complete oxidation of glycolate and other organic species from the SRAT may be necessary to minimize thermolytic hydrogen generation [5]. The glycolate oxidation may occur in the Recycle Collection Tank (RCT). The RCT heel would be adjusted with sodium hydroxide to maintain the solution caustic and sodium nitrite as corrosion inhibitor prior to the addition of condensate. The condensate can be from the contents of the Slurry Mix Evaporator Condensate Tank (SMECT) or the Offgas Condensate Tank (OGCT). The RCT collects the waste to be transferred via the Low Point Pump Pit – Recycle Pump Tank (LPPP-RPT) through a jacketed transfer-line to the Tank Farm facility. Scoping studies were performed to evaluate sodium permanganate and Fenton's reagent (i.e., iron catalyzed hydrogen peroxide) for destroying the glycolate. From the results of testing, oxidation by sodium permanganate was chosen over Fenton's reagent [6]. SRR requested corrosion testing to evaluate the materials that will be exposed to sodium permanganate, as part of a Technical Task Request (TTR) [7]. The response to the TTR is part of the Task Technical and Quality Assurance Plan (TTQAP), Task 4 – Corrosion Testing [8].

Corrosion experiments, including electrochemical and coupon immersion tests, were performed to evaluate Materials of Construction (MoC) for the RCT, jacketed transfer-line, LPPP-RPT, and the waste tanks due to the exposure of an alkaline SMECT/OGCT simulant with sodium permanganate. The jacket of the transfer-line was included as part of the evaluation in the event that there is a leak from the core pipe. No specific tests were performed for the evaporator systems. However, the results of the tests on stainless steel and the nickel based alloy (C-276) were utilized to evaluate potential impacts. The MoCs for the evaporator are either nickel based alloys or stainless steel [9]. The coupons used for testing were based on the MoC for all of these components, as listed in Table 1-1. This report presents the results of the electrochemical testing for RCT, transfer line, LPPP-RPT and the waste tanks (e.g., Tank 22) MoC at 25 and 50 ºC. An RCT simulant was used as the solution to be tested. The RCT simulant was used with and without addition of a SRAT component at different times after permanganate addition. The testing occurred immediately after, which corresponds to an hour after addition, and more than three hours after addition of permanganate. A coupon immersion test was performed for determining corrosion rates at different time intervals.

Table 1-1. Materials of construction of components impacted by permanganate

Components	Alloys
RCT	Hastelloy® C-276
Transfer-line core pipe	304L stainless steel
Transfer-line jacket pipe	A106 carbon steel
LPPP-RPT	304L stainless steel
Waste tanks	A537 carbon steel
Evaporators	304L stainless steel, Hastelloy G3 and Hastelloy G30

2.0 Background

Previous corrosion studies to assess the impact of glycolic acid/glycolate consisted of electrochemical tests, hot-wall tests and coupon exposure test performed as part of the Chemical Process Cell (CPC) flowsheet development. The study concluded that MoC of most vessels, components and piping exposure to the glycolate anion may not affect service life expectancy. However, the performance of some MoC within the DWPF CPC and feed tanks required additional testing due to the susceptibility to localized corrosion [3]. Additional accelerated electrochemical and hot-wall testing at boiling were conducted with a range of concentrations for chloride and sulfate. From this test, new Waste Acceptance Criteria (WAC) limits were determined for chloride and sulfate where susceptibility to localized corrosion was not identified [4]. Sodium permanganate additions to the RCT represent an operating condition that was not addressed in the earlier testing. The general corrosion rate for the RCT for typical processes within DWPF has been estimated to be about 1 mil per year (mpy) which is a slow, predictable rate [10].

Prior corrosion testing using sodium permanganate was performed by Wyrwas for the waste tank alternative chemical cleaning [11],[12]. A set concentration of 0.05 M sodium permanganate in caustic and acidic solutions was used for both sets of experiments. Immersion testing for a month showed corrosion rates of 0.07 mpy for American Society for Testing and Materials (ASTM) A285 carbon steel and no noticeable corrosion rate for 304L at 50 ºC in the 10 M hydroxide solution. At acidic conditions, 304L continued to have negligible corrosion rates, while A285 increased to 37.3 mpy due to pitting corrosion [12]. Electrochemical experiments of A285 at lower concentrations of hydroxide (i.e., 3 M and 5 M) showed a change in instantaneous corrosion rate (after approximately two hours of coupon immersion in solution) of 0.9 and 24 mpy on average, for 5 M and 3 M hydroxide, respectively [11].

Thus, a gap between the acidic conditions and 3 M hydroxide exists for the 0.1 – 0.2 M hydroxide range of the RCT and the waste tanks. The hydroxide concentration may be further reduced by the permanganate addition, although is not considerable since the electrochemical reaction kinetics are very slow [13].

3.0 Task Activities

Associated activities to study corrosion of the RCT, transfer line and waste tanks were documented in a Run Plan [14] that was approved by SRR prior to the start of testing. The activities were divided into two parts: A and B. Part A was dedicated to electrochemical corrosion testing of the RCT MoC and Part B focused on the electrochemical and coupon immersion testing for the MoCs of the components downstream of the RCT (i.e., transfer-line, LPPP RPT, waste tanks).

3.1 Part A. RCT electrochemical testing

The RCT and the tube bundle for the evaporator system were evaluated using electrochemical methods to determine the extent of corrosion immediately after permanganate addition and after more than three hours of permanganate addition. Testing was performed with solutions at 50 ºC, since it is the maximum operating temperature of the RCT. In addition, testing was performed with two surface treatment: freshly grounded and pre-filmed surfaces. The pre-filmed surface was prepared using a formate-based simulant to simulate the extended exposure of the RCT to formate-based residues.

3.2 Part B. Electrochemical and immersion testing of components downstream of the RCT (transfer-line, LPPP-RPT, waste tanks and the evaporator system)

The MoC for the transfer-line, LPPP-RPT, the waste tanks and the evaporator system were evaluated using the simulant after more than three hours of permanganate addition. Subparts B1 and B2 focused on the electrochemical and immersion coupon testing, respectively.

3.2.1 Part B1: Electrochemical testing for 304L and A537

Electrochemical methods were used in this part to help determine corrosion activity with exposure to simulant with permanganate. The tests were conducted at 25 and 50 ºC. The 50 ºC data was compared to the data obtained for C-276.

3.2.2 Part B2. Coupon immersion test to determine corrosion effects of A537

Immersion tests for 1 month were performed to determine environment corrosiveness and corrosion susceptibility for the MoCs of the transfer-line jacket , the evaporator system and the waste tanks. The focus was placed on localized forms of corrosion such as pitting and stress corrosion cracking (SCC). The test was performed at room temperature (i.e., temperature varied from 20 to 25 ºC since no heating sources were used).

4.0 Experimental Procedure

4.1 Materials

Materials for testing were selected based on the MoC for the RCT, transfer-line, LPPP RPT, the waste tanks, and tank farm evaporator system as displayed in Table 1-1. The RCT was fabricated using Hastelloy® C-276, which is a nickel based alloy. The transfer-line has a 304L stainless steel core pipe and an ASTM A106 grade carbon steel jacket pipe. The LPPP-RPT is made from 304L stainless steel. In addition, the waste tanks were built of ASTM A537 grade carbon steel. For the experiments, A537 grade carbon steel was used since it was readily available and was used for the transfer-line jacket (i.e., A106 grade) since the composition of carbon steel grades is essentially more than 95 wt.% iron. All the materials tested had a weld to assess the effects of welding and heat affected zones, since it may provide a more susceptible area towards corrosion. The evaporator vessels are made of either 304L stainless steel or Hastelloy® G3, which is a nickel based alloy. The MoC for the tube bundle is either Hastelloy® G3 or G30, another nickel based alloy.

For electrochemical tests, each material was cut into a 2 x 2 cm square from sample materials with different dimensions. The resulting metal square had a wire attached using silver epoxy on one side to ensure electrical connection. The metal square was cold mounted using an acrylic resin (VariDur from Buehler), so only one face was exposed to the solution to be tested. The mounted coupons were ground to a 600-grit finish prior to immersion in test solution. Figure 4-1 on the left shows a picture of the completed coupon with the exposed face.

For immersion testing, flat coupons and U-bend specimens were used. The flat coupons were obtained from a U-bend and had dimensions of approximately 1.5 x 1.0 x 0.14 inch. The U-bends consisted of a rectangular

sheet of metal 5 x 1 x 0.14 inch bent 180° around a 1-inch radius and maintained in constant strain condition with a stainless steel fastener that is electrically isolated from the metal using insulating ceramic washers. The flat coupons and U-bend were ground to a 600-grit finish which removed most of the mill-scale on the coupons. A picture of a U-bend is shown in Figure 4-1 on the right. The guidelines to make U-bends are given in ASTM G30-97 standard [15]. The U-bends were stressed to 40 lb.-inch torque using a calibrated torque wrench.

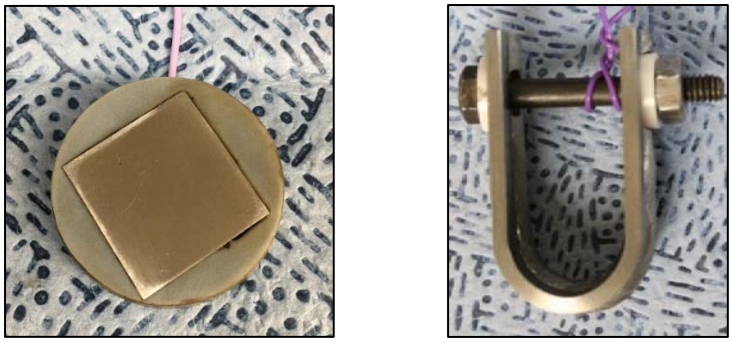

Figure 4-1. Pictures of metal coupon attached to a purple wire and mounted in acrylic (left) and stressed U-bend (right)

4.2 Simulant for testing

The simulant used represent the transfer from the SMECT condensate feed and/or the OGCT onto the RCT with heel [6]. A 50 wt.% hydroxide addition for caustic adjustment prior to addition of permanganate was poured. Table 4-1 lists the components and concentrations for the prepared simulant. The simulant was prepared using reagent grade chemicals in distilled water and, in some cases, a SRAT sludge component was included. The SRAT sludge component (identified as SB9-NG) was made in Aiken County Technology Laboratory (ACTL) and information of its constituents can be found elsewhere [16]. The SRAT sludge product contributed 125 mg of glycolate per kg of solution with additional formate, oxalate and nitrate. The nitrite and hydroxide concentrations correspond to the minimum values required by the Tank Farm WAC. The simulants will be known in the report as RCT simulant with maximum permanganate for the case without the addition of SRAT component, and as RCT simulant with SRAT when the SRAT was added.

Table 4-1. Chemical +constituents of base simulant for testing

Component(s)	Source	Formula	Concentration (M)	Final Concentration with addition of SRAT sludge (M)
Formate	Sodium Formate	$Na(CHO_2)$	0.004	0.009
Oxalate	Sodium Oxalate	$Na_2C_2O_4$	0.00022	0.00042
Nitrate	Sodium Nitrate	$NaNO_3$	0.050	0.051
Nitrite	Sodium Nitrite	$NaNO_2$	0.220	0.220
Hydroxide	Sodium Hydroxide (50wt% solution)	NaOH	0.10	0.10
Glycolate, formate, oxalate, nitrate	SRAT product (SB9-NG)	N/A	2.20 g per 1000 g Reagent Portion	N/A

Since information was not available about the optimum molar ratio of permanganate to glycolate that will reduce the glycolate concentration to less than 10 mg/kg (corresponding to the minimum detection limits), a ratio of seven moles of permanganate to one mole of glycolate was used. This value corresponded to the

highest permanganate to glycolate molar ratio that would be expected to be used in DWPF. At the time of the writing of this report, the recommended molar ratio of permanganate to glycolate was determined to be 5.7 to 1, for low and nominal glycolate concentrations [16].

Some coupons were pre-filmed with a sodium formate based simulant and the chemical composition with corresponding quantity for 2.5 L used for this test is listed in Table 4-2.

Table 4-2. Chemical composition of formate-based solution used for pre-film coupon

Chemical	Quantity (g)
Sodium Oxalate ($Na_2C_2O_4$)	14.46275
Mercury Nitrate ($Hg(NO_3)_2.H_2O$	1.2795
Manganese Nitrate (50 wt.% $Mn(NO_3)_2$ + 5 wt.% HNO_3) - liquid	49.646
Rhodium Nitrate (4.933 wt.% Solution) – liquid	0.46675
Zirconium Nitrate ($ZrO(NO_3)_2.6H_2O$)	0.21
Sodium Sulfate (Na_2SO_4)	15.52625
Sodium Chloride (NaCl)	4.9945
Aluminum Nitrate ($Al(NO_3)_3.9H_2O$)	7.525
Sodium Nitrate ($NaNO_3$)	111.5325
Sodium Formate ($NaC_2H_3O_3$)	213.00675
Magnesium Nitrate ($Mg(NO_3)_2.6H_2O$)	5.354
Iron Nitrate ($Fe(NO_3)_3.9H_2O$)	2.541
Nickel Nitrate ($Ni(NO_3)_2.6H_2O$)	1.23875
Potassium Nitrate (KNO_3)	2.072
Calcium Nitrate ($Ca(NO_3)_2.4H_2O$)	1.60575

4.3 Test setup

4.3.1 Electrochemical Testing

A standard corrosion cell was used, and a picture is presented in Figure 4-2 on the left. The cell was placed on top of a hotplate/stirrer for temperature control and to stir the simulant. A three-electrode system was used to perform electrochemical experiments: reference electrode, counter electrode and working electrode. The reference electrode consisted of a saturated calomel electrode (SCE) placed in a salt bridge made of glass with frit at the tip to minimize disturbances in the electrode when the solution was heated while maintaining electrical continuity. Prior to each test, the electrode was checked against a standard (a SCE in saturated KCl solution that was not used for testing). The counter electrode consisted of two graphite rods electrically connected with a wire; a working electrode was the mounted coupon placed in a glass holder.

A picture of the glass holder with a mounted coupon is shown also in Figure 4-2 on the right. A solution volume of 500 mL was used, and the holder was adjusted until the mounted coupon was fully immersed.

The electrochemical testing method was performed with a potentiostat (Gamry Instruments) and consisted of Open Circuit Potential (OCP) measurement, Linear Polarization Resistance (LPR) and Cyclic Potentiodynamic Polarization (CPP). The OCP monitoring measured the potential until reaching steady state conditions (i.e., disturbances in the potential where less than 5 mV/min), usually between two to three hours. Then, an LPR was performed, in duplicate with a 10-minute OCP stabilization period in between. The LPR test, based on ASTM G59 [17], polarizes the sample to +/- 30 mV vs. OCP at a rate of 0.167 mV/s and the resulting linear response is used to determine the corrosion current density using Faraday's Law.

The CPP experiment was performed, after another 10-minute OCP stabilization period. The CPP technique is based on ASTM G61[18] and provides information regarding corrosiveness of the solution for the MoC as well as information on susceptibility towards localized corrosion. The CPP was performed by scanning the potential and obtaining the current response starting at -0.05 V vs. OCP up until the potential where the limiting current density reached 1 mA/cm^2 (less than 2 V vs. SCE), at a rate of 0.167 mV/s, then the potential was reversed until OCP. Appendix A describes the OCP, LPR and CPP tests tailored to this discussion and data obtained from these tests.

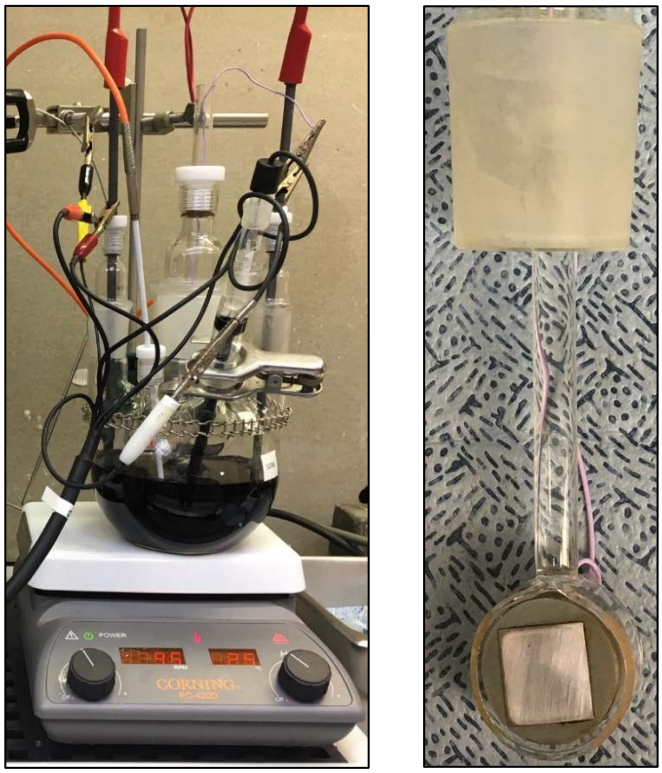

Figure 4-2. Pictures of a glass corrosion cell on top of a hotplate/stirrer (left) and mounted coupon in glass sample holder (right)

Studies by Mickalonis [4] showed the appearance of an adherent film on C-276 when using formate-based simulants. The use of a pre-filmed coupon from a formate-based simulant was used to test a surface that may more closely resemble a surface after long term formate exposure. (i.e., 20+ years of operation for the RCT). To develop the pre-filmed surface, the coupons were to be immersed in a boiling solution for up to two weeks. However, after two weeks, there was not a visible film present. It was decided then to use a

galvanostatic method to develop the film for a faster approach. To develop the film on the coupon for study, a galvanostatic experiment of 4 mA/cm^2 for 5 minutes was performed after an OCP monitoring for 1 hour. The resulting film can be observed in a picture of the coupon after the galvanostatic experiment in Figure 4-3 (a). Analysis of this film by X-Ray Diffraction (XRD) showed taenite (Fe, Ni) with minor calcite peaks (Figure 4-3 (c)). Two scratches made on the surface of the layer (white/yellow parallel lines) showed that the film had an approximate thickness of 1 µm, when measuring approximate depths using a Laser Confocal Microscope (LCM), (Figure 4-3 (b)).

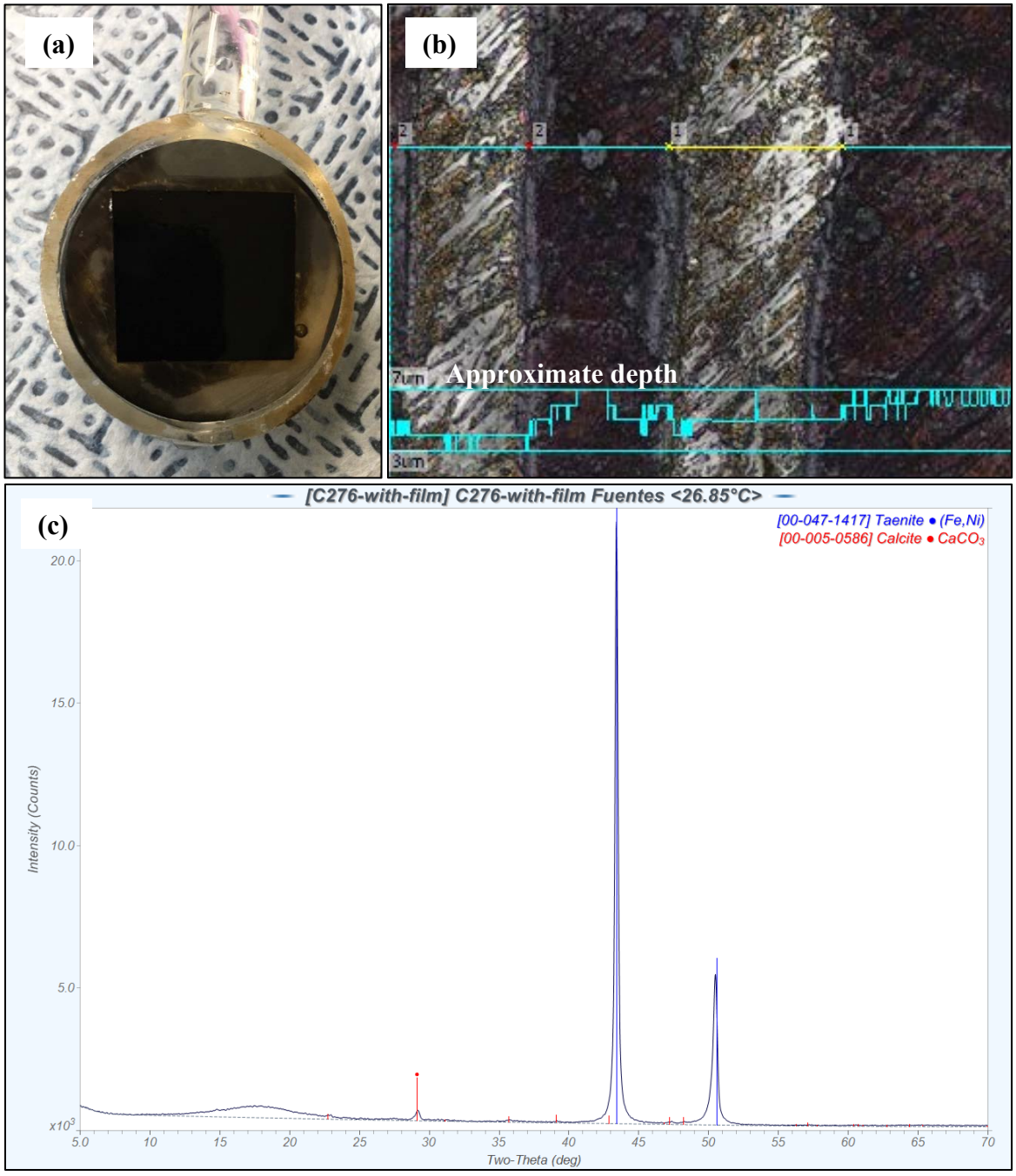

Figure 4-3. (a) Picture of the coupon after galvanostatic test, (b) Laser Confocal Microscope picture for obtaining the film thickness and, (c) X-Ray Diffraction spectrum of the film on C-276 coupon

4.3.2 Immersion Testing

A large glass vessel was used with 6 L of simulant for immersion testing. Figure 4-4 shows a picture of the vessel with the coupons that were placed initially. The volume selected was based on the guidelines provided in ASTM G31 [19] which states that the preferred minimum ratio of test solution volume to specimen surface area is 0.20 mL/mm^2. The glass vessel was placed in a secondary container and there was no temperature control, so the temperature of the test corresponded to room temperature (i.e., 22 to 25 ºC). U-bend coupons were maintained in solution for four weeks.

A planned interval removal test was performed using flat coupons and is presented in Table 4-3. Four coupons were exposed for 1 week and one coupon each for three and four weeks. The corrosion rates correspond to A1, A3, A4 and B at different time intervals. A1 was obtained as an average of three coupons to account for variability in the corrosion rate within the first week. For A3 and A4, only one coupon was exposed. A2 is the calculated difference in the corrosion rates for A4 and A3. For B, a coupon was inserted into the test solution at the end of the third week and was removed after the fourth and last week. The corrosion rates of A1, A3, A4, and B are obtained by determining the mass lost during the time they were immersed.

Table 4-4 shows the criteria for the evaluation of the mass loss in terms of the environment corrosiveness and/or alloy corrodibility. When B = A1, the corrosivity of the environment has not changed after 3 weeks of exposure. On the other hand, if B < A1 the corrosivity has decreased or if B > A1 it has increased. Corrosion rate A2 evaluates the corrodibility of the alloy after three weeks of exposure. When A2 = B, the alloy corrodibility has not changed. In contrast, if A2 < B the corrodibility has decreased, and when A2 > B it has increased. The environment corrosiveness is based on the solution changing the corrosive nature and becoming more aggressive or passive (first week compared to fourth and last week) . The alloy corrodibility compares the alloy propensity to corrode during the same time period (last week).

Figure 4-4. Picture of glass vessel for immersion test with initial coupons

Table 4-3. Interval Coupon Test

Coupon				
	A1			
1, 2, 3				
			A3	A2
4				
				A4
6				
				B
5				
	1	2	3	4
	Time (weeks)			

Table 4-4. Criteria for evaluating environment corrosiveness and alloy corrodibility

Criteria	Environment Corrosiveness	Criteria	Alloy Corrodibility
B = A1	Unchanged	A2 = B	Unchanged
B < A1	Decreased	A2 < B	Decreased
B > A1	Increased	A2 > B	Increased

4.4 Quality Assurance

The TTR for this work specified the testing has a functional class of Safety Class. Requirements for performing reviews of technical reports and the extent of review are established in manual E7 2.60. SRNL documents the extent and type of review using the SRNL Technical Report Design Checklist contained in WSRC-IM-2002-00011, Rev. 2. The supporting data from the experiments was posted in Electronic Laboratory Notebook G8519-00191-05. The planning, test protocols, and data review per WSRC-IM-2002-00011 Rev. 2 are compliant with the requirements for Safety Class data collection.

5.0 Results and Discussion

The corrosion testing results are divided into two sections. The first section involves the electrochemical testing of MoC for RCT and the tank farm evaporator system. The second section presents the corrosion testing on MoCs for the transfer-line, evaporator system, and waste tanks and is divided into two parts: electrochemical testing and immersion testing.

5.1 Part A. Electrochemical testing of MoC for the RCT (Hastelloy® C-276)

Electrochemical tests were performed using mounted coupons of C-276 with a freshly ground surface. At first, the OCP was recorded until it reached steady state condition. Once the OCP value was stable, a 20 wt.% sodium permanganate solution was added to the corrosion vessel at a rate of 0.18 mL/min using a syringe pump. The addition was planned to last approximately 20 minutes (3.57 mL in total). LPR experiments were then performed (after a 40 minute wait for the OCP to stabilize again) to measure a corrosion current density during the period when the permanganate is most reactive. Figure 5-1 shows an example of OCP stabilizing for C-276 exposed to RCT simulant with maximum permanganate. As observed, the potential started at a negative value (-0.273 V vs. SCE) and when the permanganate was added slowly,

the potential shifted to a positive value instantly and then gradually started to reach a plateau (around 0.330 V vs SCE). The shift in potential is due to a change in oxidative conditions from the addition of permanganate in solution and was observed in all the tests.

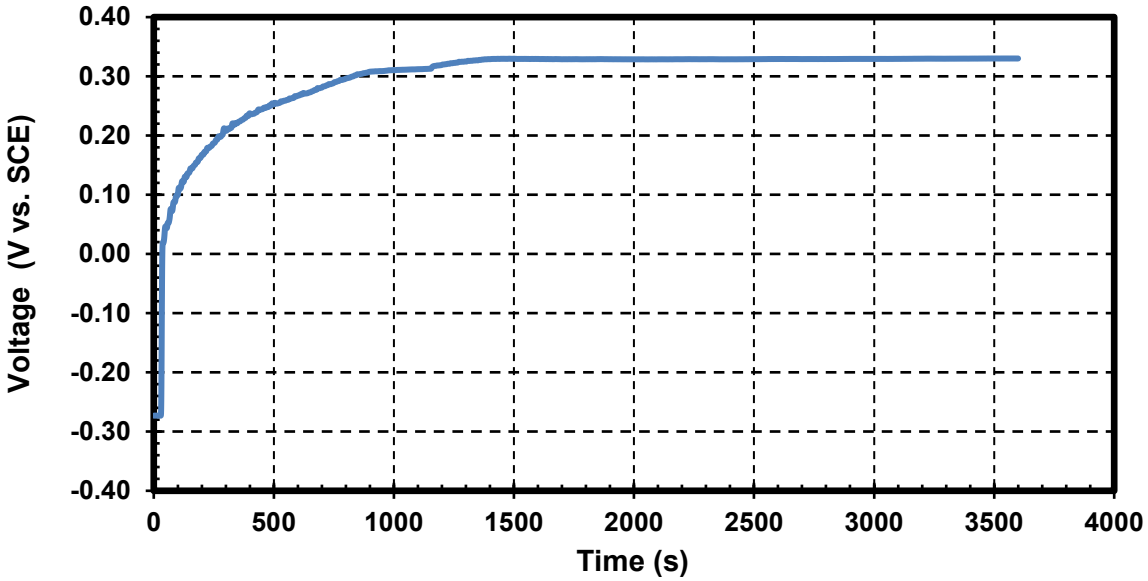

Figure 5-1. OCP measurement of Hastelloy® C-276 with a freshly ground surface during permanganate addition in RCT simulant with maximum permanganate at 50 ºC

CPP experiments for C-276 were performed immediately after permanganate addition (i.e., approximately one hour after the last drop of permanganate was added) and are presented in Figure 5-2 for a freshly ground and pre-filmed surface in the two simulants. Experiments were also performed using a simulant after more than three hours and are shown in Figure 5-3 for a freshly ground surface. The OCP started at potentials greater than 166 mV vs. SCE, that are over 400 mV greater than the hydrogen evolution reaction (HER) starting potential (HER potential becomes more negative at higher pH) indicating high oxidation conditions, shown for illustration purposes in Figure 5-3. The CPP curves are more similar for a freshly ground surface compared to pre-filmed surface, independent of permanganate addition. This may correspond to the interaction of permanganate at the surface of coupons that dominate the CPP curve response.

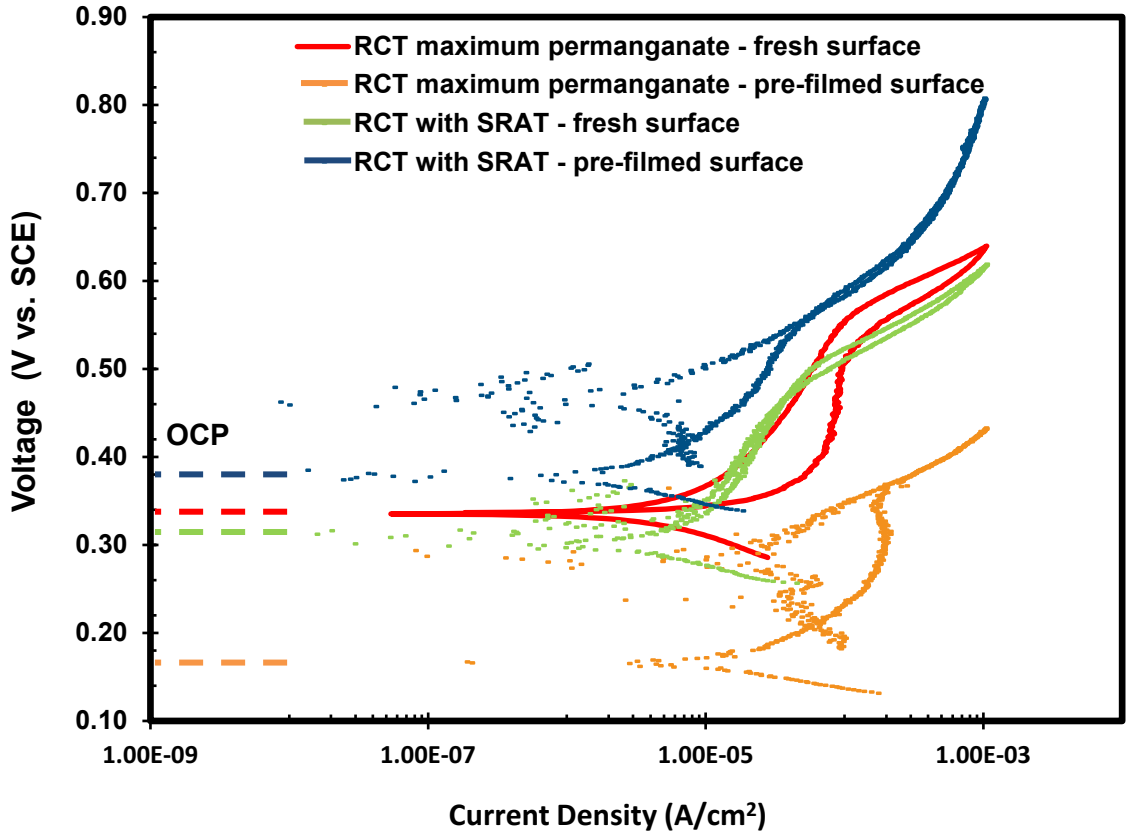

Figure 5-2. CPP results of Hastelloy® C-276 for testing performed immediately after permanganate addition at 50 °C

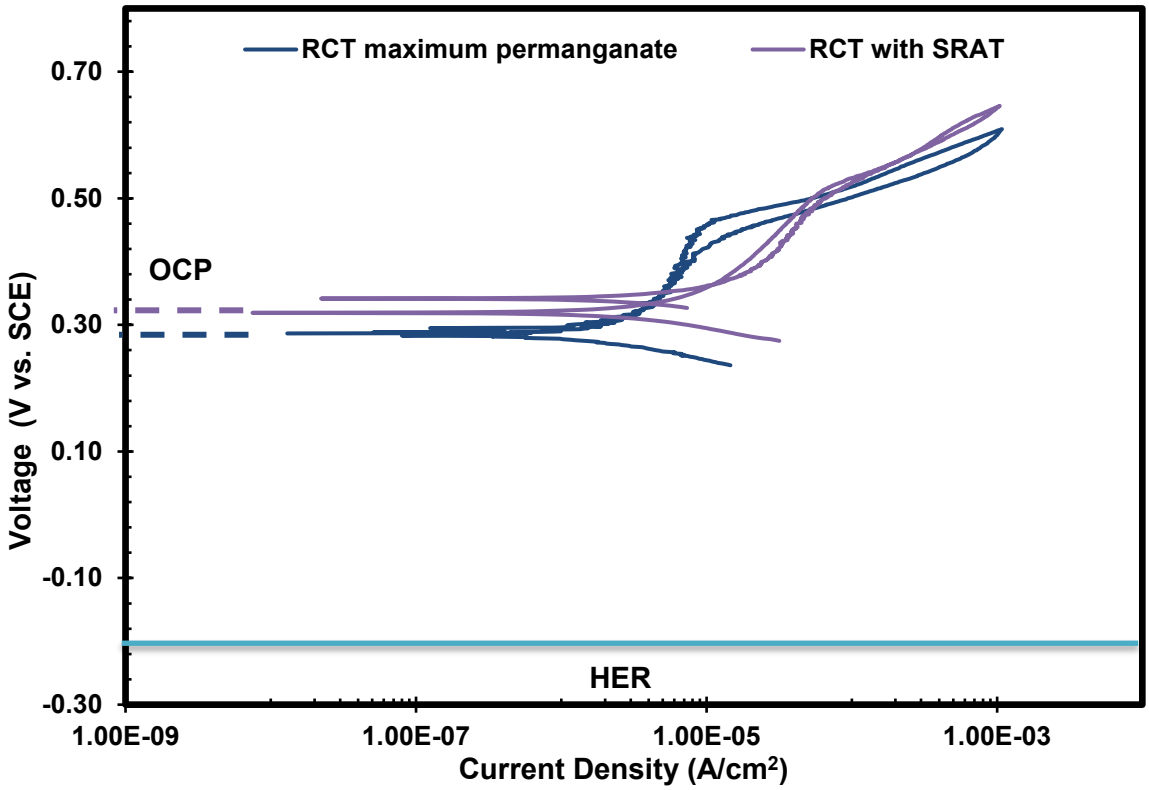

Figure 5-3. CPP results of Hastelloy® C-276 for testing performed more than three hours after permanganate addition at 50 ºC

There was no passivation region observed in the CPP curves, except for testing more than three hours after addition for a freshly ground surface exposed to RCT simulant with maximum permanganate (Figure 5-3). The appearance of the passive region may indicate that the permanganate oxidation reaction has decreased in kinetics and may not dominate the CPP response.

The OCPs, passivation current densities (i_{pass}) and cross-over potentials (E_{CO}), if obtained, from CPP experiments are listed in Table 5-1; as well as total current densities (i_{total}) obtained from two LPR analyses for each surface in the corresponding simulant at 50 ºC. Comparing the values for OCPs shows that experiments with a freshly ground surface were obtained in a range corresponding from 283 to 335 mV vs. SCE. More than three hours after permanganate addition, the CPP also showed a similar range. For the pre-filmed coupons, the lowest and highest values of OCPs (i.e., 166 and 376 mV vs. SCE) and of current limit potentials (i.e., the potential where current limit of 1 mA/cm^2 is reached) from all the tests performed were achieved. Since the pre-film properties on the coupon before and after the test were not analyzed thoroughly since it did not seem to be necessary to relate CPP response with layer condition, it is not clear the reason that two distinct CPP responses were obtained. The highly positive OCP observed appears to be independent of surface and solution conditions.

Corrosion current density is usually obtained from LPR by polarizing the sample at a small potential range between OCP. Since active permanganate oxidation is occurring (thus affecting the OCP as observed in Figure 5-1), the total current density term is introduced. The total current density is the sum of permanganate oxidation electrochemical reaction and corrosion current densities. The total current densities obtained were

about 42.3 and 56.7 μA/cm^2, corresponding to the RCT simulant with maximum permanganate for freshly ground surface and pre-filmed surface, respectively. This is reflective of active permanganate oxidation and the increase in current density for the pre-filmed surface may also add additional electrochemical reactions of permanganate with the formate-based layer. The total current densities were lower than 11.6 μA/cm^2 for RCT with SRAT simulant and simulants tested more than three hours after permanganate addition independent of surface preparation. This reduction in current density may indicate that as the permanganate oxidation reduces, the reaction current densities decrease from the total current density and the corrosion current density becomes more significant.

Table 5-1. Electrochemical parameters obtained from CPP and LPR experiments for Hastelloy® C-276 at 50 ºC

Surface Condition	Simulant	$i_{total,}$ μA/cm^2	OCP, V vs. SCE	i_{pass}, μA/cm^2	E_{CO}, V vs. SCE	Hysteresis
Freshly ground surface (600 grit ground)	RCT with mp[1]- immediately after addition	42.3	0.335	N/A	0.34	Positive Closed Loop
	RCT with SRAT- immediately after addition	10.1	0.301	N/A	0.47	Positive Closed Loop
	RCT with mp[1]- after addition for more than three hours	2.9	0.283	5.7	N/A	Mixed
	RCT with SRAT- after addition for more than three hours	4.5	0.319	N/A	N/A	Mixed
Pre-filmed surface	RCT with mp[1]- immediately after addition	56.7	0.166	N/A	N/A	Negative
	RCT with SRAT- immediately after addition	11.6	0.376	N/A	N/A	Negative

[1]indicates maximum permanganate addition

Pictures after test are presented in Figure 5-4. The pictures show the appearance of a layer for the cases when the coupon had a freshly ground surface preparation. The appearance of this layer seems to be less

uniform for the tests performed immediately after permanganate addition. The pre-filmed surface was a black coating and pictures after tests showed that the layer produced does not change significantly in appearance, although some delaminating instances were seen at the corners. Correlating these pictures, with the hystereses of the CPP curves presented in Figures 5-2 and 5-3 and named in Table 5-1, non-uniform layers were observed for CPP results with positive closed loops hystereses (i.e., CPP tests using freshly ground surface specimens tested immediately after permanganate addition). The resulting layer formed on the coupons has been identified as an amorphous mixture of manganese oxides by other researchers [20]. The pictures for C-276 long after (i.e., after more than three hours) permanganate addition (Figure 5-4) shows a thin layer and may provide an indication that metal activity reaction with permanganate was lower. The pre-filmed coupons CPP curves showed negative hystereses (Figure 5-2) with no significant changes in this film. After removing the film or layer from the surface of all coupons, there were no underlying pits observed in any of them. Since a layer was developed on the coupons during testing, the CPP response, as mixed (characteristic of a localized corrosion borderline case) and positive closed loop hystereses, may indicate film degradation or thickening of the adherent film.

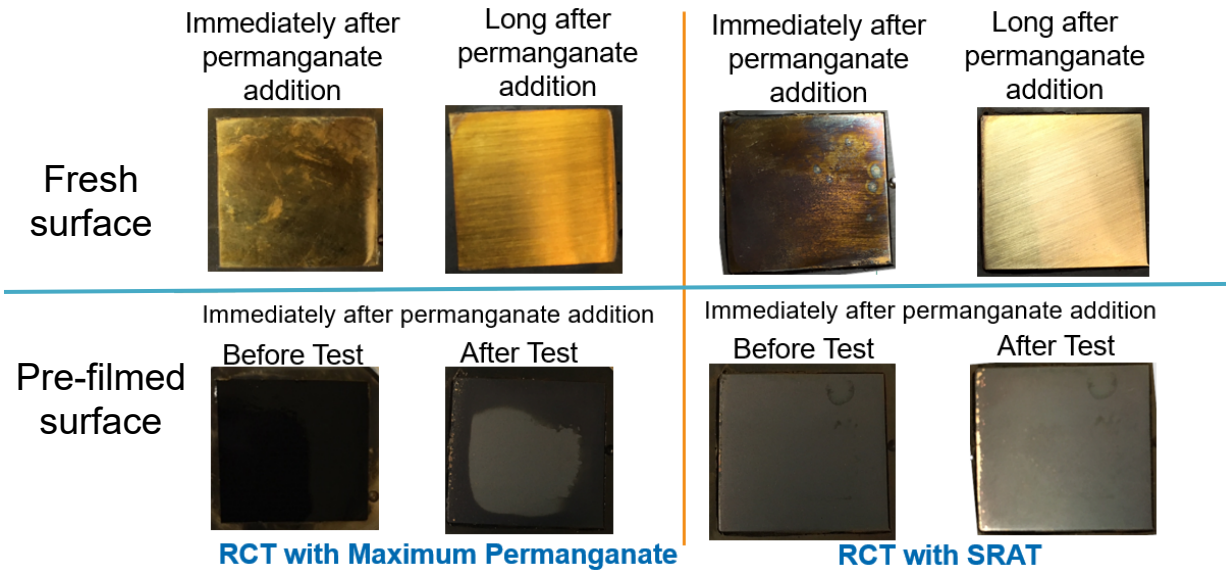

Figure 5-4. Pictures of Hastelloy® C-276 for freshly ground surface after experiment and pre-filmed coupons before and after experiment

An electrochemical experiment using platinum was performed since platinum can be used to detect current due to electrochemical reactions that are occurring at the surface, rather than metal dissolution and it is not susceptible to localized corrosion. The experiment using platinum was needed to support the hypothesis that a high current was being recorded due to the permanganate oxidation reaction. Platinum was placed in a polytetrafluoroethylene (PTFE) holder for corrosion coupons that shows the platinum through a circular window of 1 cm^2 surface area (Figure 5-6). An experiment was performed using the RCT simulant with maximum permanganate where it was tested immediately after the permanganate was added. Table 5-2 lists the electrochemical parameters obtained from LPR and CPP for platinum. The CPP curve is presented in Figure 5-5.

Table 5-2. Electrochemical parameters obtained from CPP and LPR experiments for platinum

Metal	Simulant	i_{total}, µA/cm²	OCP, V vs. SCE	i_{pass}, µA/cm²	E_{CO}, V vs. SCE	Hysteresis
Platinum	**RCT with mp[1]-immediately after addition**	37.6	0.243	N/A	0.253	Positive Closed Loop

[1]indicates maximum permanganate addition

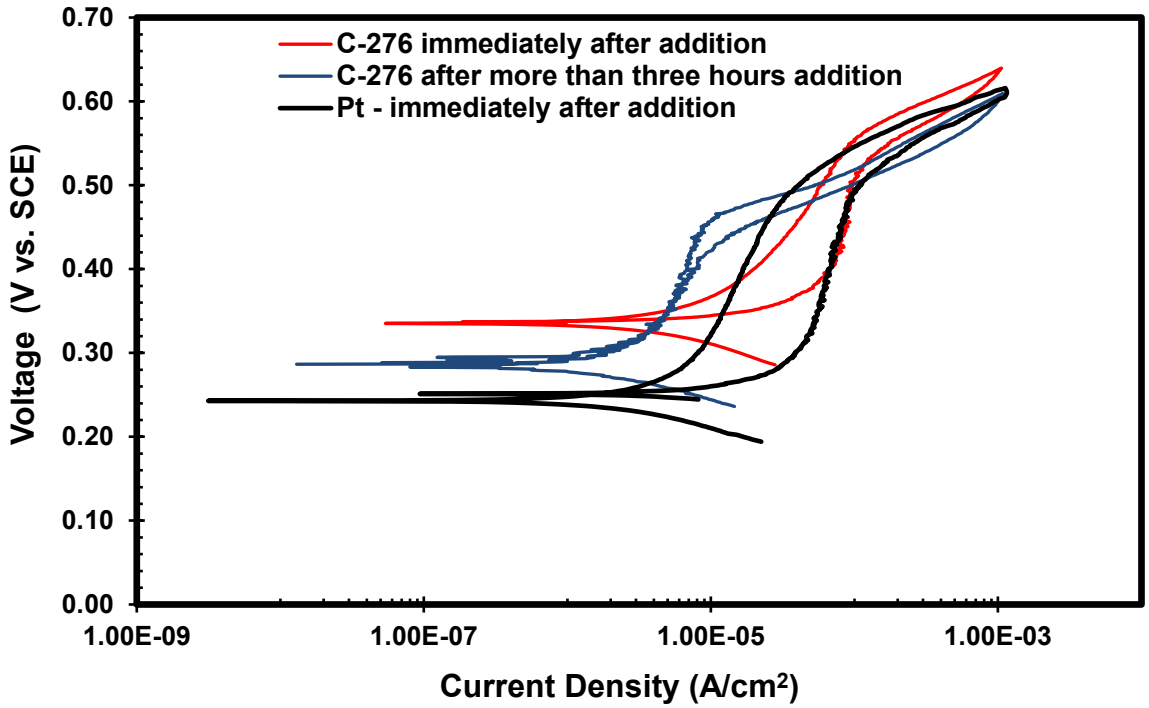

Figure 5-5. CPP results of C-276 and platinum in RCT simulant with maximum permanganate tested immediately after and C-276 after more than three hours of permanganate addition at 50 ºC

For platinum, the total current density obtained was 37.6 µA/cm², which is similar to the total current density obtained for C-276 (i.e., 42.3 µA/cm²) with a freshly ground surface at similar conditions. The CPP result for platinum (Figure 5-5) shows a positive closed loop hysteresis with a cross-over potential close to OCP (E_{CO} – OCP = 0.01 V), similar to what was observed for C-276 at similar solution conditions, albeit different OCPs indicating similar hysteresis response. Figure 5-5 also shows the CPP curve of C-276 after addition in which a passive region was observed and passive current density was determined, as listed in Table 5-1.

The pictures for platinum before and after, presented in Figure 5-6, has a comparable layer with C-276 immediately after adding permanganate that also stained the PTFE holder. The results of the CPP for platinum, comparable to C-276, provides confirmation that activity recorded was due to the electrochemical activity of permanganate oxidation, and was the cause of the surface layer formed on the surface. The positive closed loop hysteresis may correspond to film thickening, since a passive region was not observed. After removing the layer of all the coupons, no corrosion attack was observed indicating that after driving the potentials to high oxidizing conditions, the material was not susceptible to localized corrosion. The absence of any type of corrosion attack after polarization to high potentials indicate that the material is not

susceptible to localized corrosion when exposed to these simulants. Additional information can be provided by performing a Cyclic Voltammetry (CV) experiment to establish the different mechanisms of permanganate oxidation and to be able to separate them from metal dissolution.

Figure 5-6. Pictures of platinum in PTFE holder before and after test

5.2 Part B. Corrosion Tests of MoC for transfer pipe, evaporator system, and the waste tanks

The corrosion tests for this part are divided into two sections: the electrochemical test and the immersion test. The electrochemical tests were performed initially to determine the conditions for the immersion coupon testing and will be explained in detail.

5.2.1 Part B1. Electrochemical Corrosion Tests

Electrochemical experiments were performed using the RCT with maximum permanganate and RCT with SRAT simulants after having permanganate in the simulants for more than three hours. Table 5-3 lists values obtained by running LPR and CPP experiments. The total current densities obtained were 1.4 $\mu A/cm^2$ or less for both alloys in both solutions tested at 25 ºC and increased at higher temperature. The low current densities, compared to C-276 (Table 5-1) and platinum (Table 5-2), may indicate that the current density related to permanganate oxidation is reduced with time and the corrosion current may have a more significant impact for the total current density. At 50 ºC, the total current densities were higher for each alloy exposed to the RCT simulant with maximum permanganate than RCT with SRAT. The high total current density at temperature indicates higher kinetics for electrochemical reactions including corrosion.

The CPP curves for A537 and 304L are presented in Figures 5-7 and 5-8, respectively. The OCPs were about the same range as observed for C-276 (Figures. 5-2 and 5-3) and even platinum (Figure 5-5). However, for these alloys, which are iron based, there was a passive range observed in all cases and a passivation current can be extracted from it. The passive current density, in most cases, was higher at 50 than 25 ºC, indicative of electrochemical reaction kinetics increasing with temperature. Additionally, the hysteresis of the CPP curve was negative in most tests, except for two tests which were mixed.

Table 5-3. Electrochemical parameters obtained from CPP and LPR experiments for A537 carbon steel and 304L stainless steel

Metal	Simulant	Temp.[2], °C	i_{total}, µA/cm^2	OCP, V vs. SCE	i_{pass}, µA/cm^2	E_{CO}, V vs. SCE	Hysteresis	Corrosion rates, mpy
A537 Carbon Steel	RCT with mp[1]-after addition for more than three hours	25	0.8	0.252	4.1	0.509	Negative	0.38
		50	8.9	0.299	16.2	N/A	Mixed	4.16*
	RCT with SRAT-after addition for more than three hours	25	1.4	0.183	3.8	0.577	Negative	0.67
		50	6.6	0.274	14.3	0.586	Negative	3.11*
304 L Stainless Steel	RCT with mp[1]- after addition for more than three hours	25	0.7	0.168	22	N/A	Mixed	0.29
		50	3.3	0.302	11.4	0.559	Negative	1.34*
	RCT with SRAT-after addition for more than three hours	25	0.8	0.203	5.2	0.555	Negative	0.32
		50	1.2	0.114	5.5	0.539	Negative	0.49*

[1]indicates maximum permanganate addition
[2]Temperature
*Not applicable for the operating temperatures of the transfer-line, LPPP-RPT and Tank 22

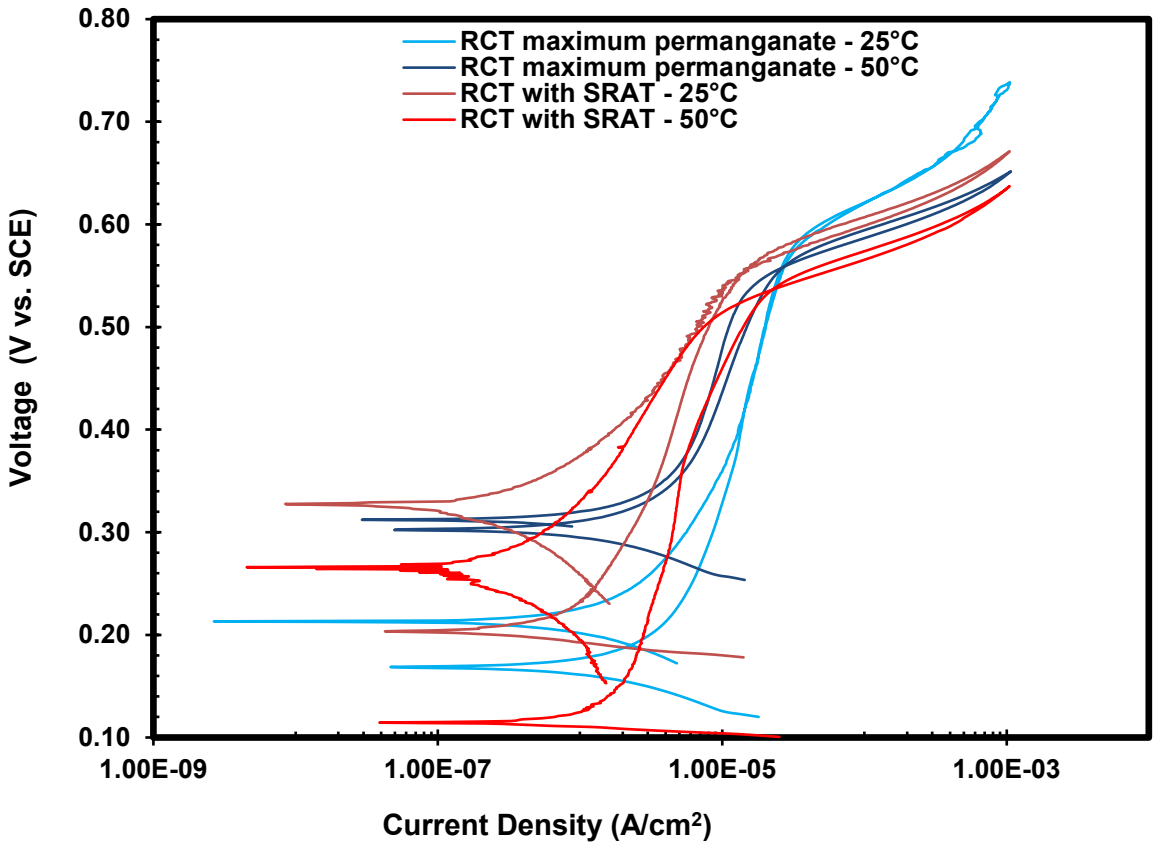

Figure 5-7. CPP results of A537 carbon steel for testing performed with two simulants at 25 and 50 ºC

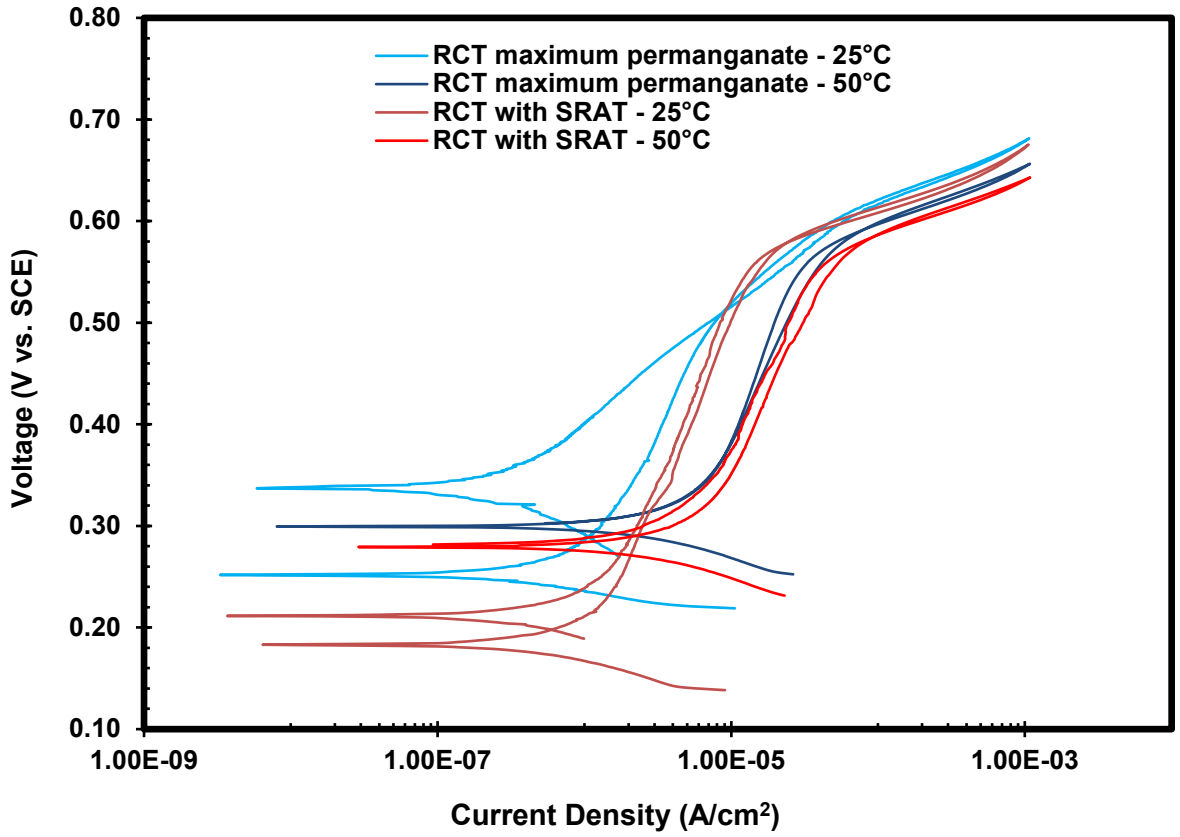

Figure 5-8. CPP results of 304L stainless steel for testing performed with two simulants at 25 and 50 ºC

Images of the coupons after testing are shown in Figure 5-9. The pictures show the appearance of a multicolored layer, specially at 25 ºC for the alloys exposed to RCT simulant with maximum permanganate. The layer seems to be less prominent at 25 ºC for the simulant with SRAT. The layers do not appear to be very uniform, compared to the layers obtained for C-276 (Figure 5-4). However, lack of uniformity may be due to thickness and optical differences that were not studied in this report. The multicolor structure, observed in more definition at 25 ºC, may also be an indication of a thinner film compared to the surfaces at 50 ºC for RCT simulant with maximum permanganate.

The underlying metal did not show any pits or corrosion correlating with mostly negative hystereses response. The appearance of passive regions in the CPP is used to determine metal susceptibility towards localized corrosion and provides additional confirmation that permanganate oxidation reactions are reduced. The permanganate oxidation reactions were assumed to be negligible, so corrosion current density can be equal to the total current densities, obtained by LPRs, and corrosion rates were calculated as shown in Table 5-3.

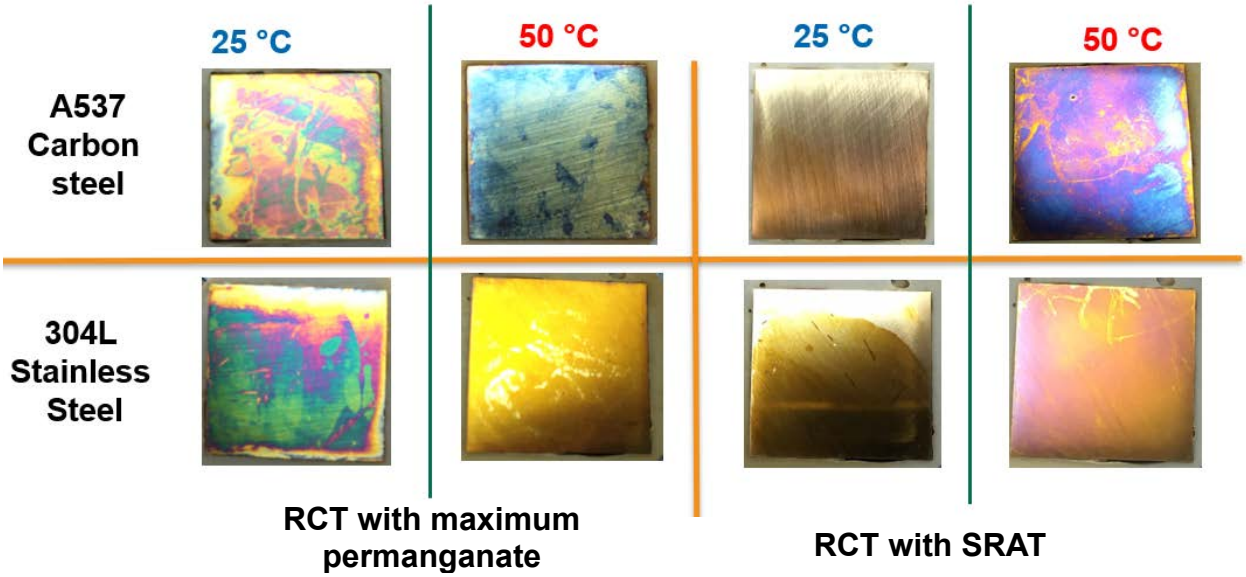

Figure 5-9. Pictures of A537 carbon steel and 304L stainless steel coupons after test at 25 and 50 ºC

5.2.2 Part B2. Immersion Coupon Corrosion Test

Immersion tests were performed using the RCT simulant with maximum permanganate. This simulant was chosen after performing electrochemical test for A537 carbon steel and noticing high current densities, specially at 50 ºC, based on LPR results. In addition, A537 can be more susceptible towards localized corrosion such as pitting and SCC in comparison to the other two alloys: 304L and C-276. The immersion test provides long term corrosion exposure, especially for identifying localized corrosion such as pitting and SCC.

The immersion test was performed using six flat welded coupons that were removed at different intervals and two U-bend coupons removed after four weeks. Figure 5-10 shows pictures of the setup after the initial and final weeks with a close-up of the glass vessel at the final week showing the appearance of a multicolor layer. The multicolor layer disappeared after several weeks indicating that this film can degrade with time. The appearance of a similar layer was also observed after removing a coupon from solution at each interval and at the end of testing. Pictures of a flat coupon and U-bend after four-week exposure are displayed in Figure 5-11. The layer that was observed on the coupon and on the glass have very similar hues. In addition, this layer was instantly removed just by immersing the coupon in 1 M HCl solution. After cleaning, all the coupons had a very similar appearance as before they were immersed with no signs of localized corrosion including pitting and SCC for the stressed specimens. All other coupons removed are shown in Appendix B and none of the coupons showed any signs of general or localized corrosion.

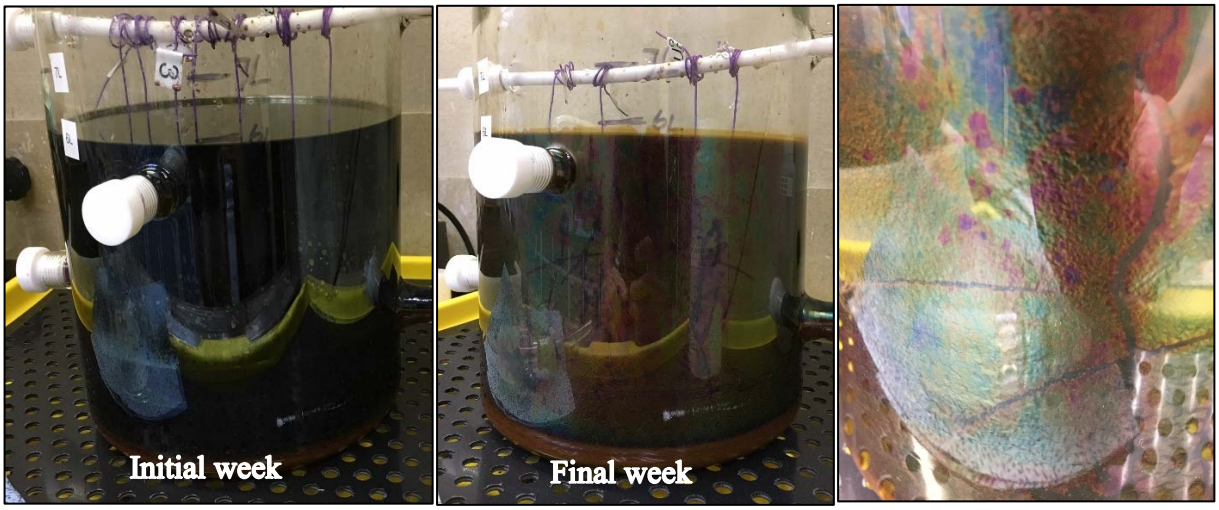

Figure 5-10. Immersion Test Setup pictures at starting and ending of test. A close-up of the vessel at the end of testing shows a multicolor layer adhered to the glass (far right picture).

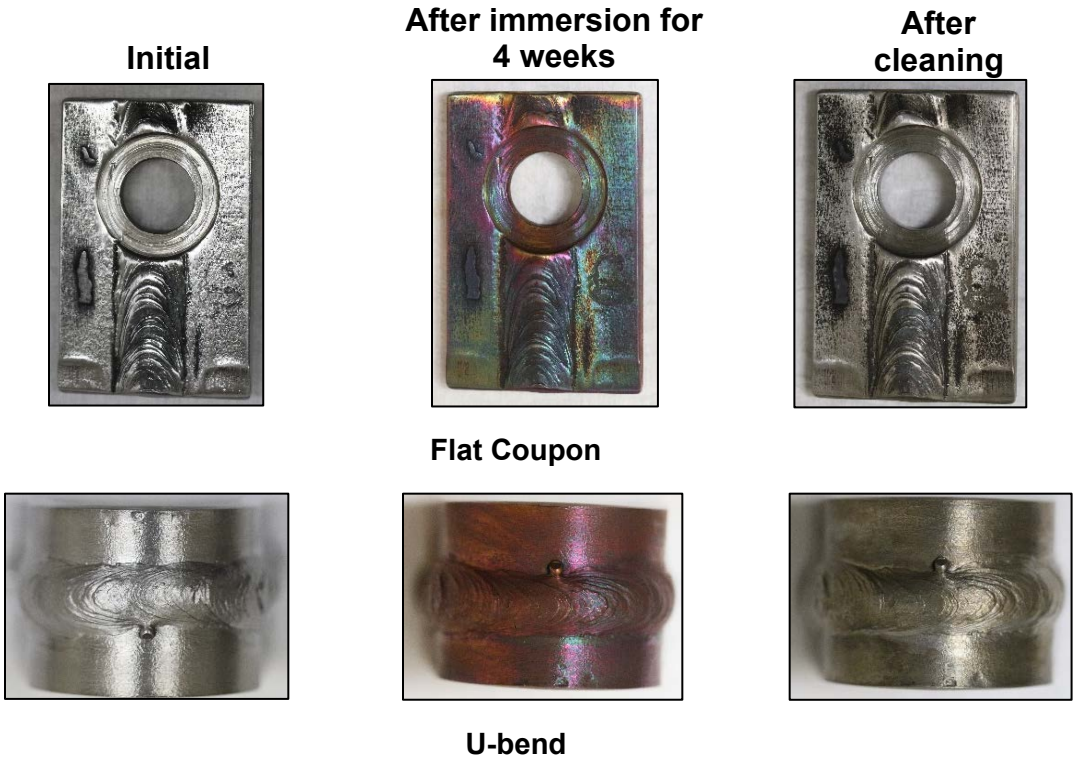

Figure 5-11. Pictures of a flat coupon and stressed U-bend: initially, after being immersed for four weeks and after cleaning with 1 M HCl solution

The mass-loss based corrosion rate was obtained by weighing the coupon initially and then after each planned removal and cleaning. The results are listed in Table 5-4 for flat welded coupons and Table 5-5 for U-bend welded coupons. Surface area was obtained for each coupon using calibrated calipers and are also listed in the tables. The weld surface was obtained assuming a cylinder in the middle of the rectangular coupon. All the coupons reflected a mass gain after the test with a maximum mass gain of 2.1 mg after only

one week of immersion. After cleaning the coupons with 1 M HCl, none of the coupons showed appearance of general corrosion and the masses of the samples do not reflect a significant mass loss. The corrosion rate was calculated in mpy in accordance with ASTM G31[19], using equation 1,

$$\text{Corrosion Rate} = (K \times W)/(A \times T \times \rho) \quad (1)$$

where, K is a conversion constant, 3.45×10^6, for mpy, W is the mass loss in grams, A is the surface area in cm^2, T is the exposure time in hours, and ρ is the density in grams/cm^3.

For the three coupons removed after 1 week, the corrosion rate was 0.39 mpy on average with a standard deviation of +/- 0.02 mpy and about 0.05 to 0.18 mpy, for the coupons removed after three and four weeks, respectively. Corrosion rates after the first week are comparable to the instantaneous corrosion rates using LPR obtained for A537 and 304L mostly at 25 ºC (Table 5-3).

Using the criteria from Table 4-3, essentially B = A1 (i.e., average of corrosion rate for coupons 1, 2 and 3 is similar to corrosion rate for coupon 5), indicates the environment corrosiveness remains unchanged. In addition, A2 = B (i.e., the corrosion rate difference between coupon 6 and coupon 4 is 0.13 mpy compared to coupon 6 which at rates lower than 1 mpy can be regarded as a slow rate and assumed negligible) specifying that alloy corrodibility is unchanged. Corrosion rates for the U-bend were about 0.08 mpy on average and conforms to a low corrosion rate.

Table 5-4. Coupon surface area and weight changes of flat welded coupons after immersion and cleaning to determine corrosion rate

Coupons	Corrosion rate identifier	Surface Area of coupon, cm^2	Removal period, week	Initial weight, g	Mass gained, g	Weight after cleaning, g	Mass loss, g	Corrosion rate, mpy
1	**A1**	22.96	1	28.9317	0.0021	28.9283	0.0034	0.39
2		22.64	1	30.0536	0.0010	30.0502	0.0034	0.40
3		22.96	1	28.6847	0.0018	28.6815	0.0032	0.37
4	**A3**	22.17	3	25.1999	0.0013	25.1987	0.0012	0.05
5	**B**	22.69	1	27.2000	0.0000	27.1969	0.0031	0.36
6	**A4**	23.10	4	28.7223	0.0017	28.7160	0.0063	0.18

Table 5-5. Coupon surface area and weight changes of U-bend welded coupons after immersion and cleaning to determine corrosion rate

U-bend coupons	Surface Area of coupon, cm^2	Removal period, week	Initial weight, g	Mass gained, g	Weight after cleaning, g	Mass loss, g	Corrosion rate, mpy
228	73.90	4 weeks	101.1162	0.0043	101.1047	0.0115	0.10
230	74.09	4 weeks	99.3826	0.0052	99.3764	0.0062	0.06

6.0 Conclusions

The results of this corrosion study using simulants based on RCT simulant with maximum permanganate and with SRAT component (includes glycolate) tested at different times after adding sodium permanganate (immediately and after more than three hours) showed that accelerated corrosion is not expected for MoCs

for the RCT, transfer line, LPPP-RPT, the tank farm waste tanks or evaporator systems. Although specific tests for the evaporator were not performed, it is expected that given the anticipated environments (i.e., permanganate and hydroxide concentrations, temperatures) and the similar behavior of the stainless steel and nickel based alloys, that no accelerated corrosion will occur in these vessels due to the glycolic destruction activity.

Electrochemical tests were successful in determining the instantaneous corrosion rate when the activity of the permanganate oxidation reaction was low (after three hours of addition). The calculated instantaneous corrosion rate (obtained from LPR) was 0.38 mpy for A537 and 0.29 mpy for 304L and were comparable to corrosion rates obtained after coupon immersion for 1 week (0.39 mpy on average) at similar conditions. LPR tests using simulant with SRAT component added showed lower current densities than RCT simulant with maximum permanganate (without SRAT component) due to the decrease in permanganate oxidation activity since glycolate in the solution reacts with some of the permanganate during the initial addition of 20 minutes. Since some tests were performed when permanganate addition was most active (i.e., during the first three hours of addition for C-276 and platinum), the electrochemical activity of the permanganate was a contributing factor for the current density measured by LPR. The appearance of a layer on the surface also confirms the permanganate activity and when removed the surface was pristine with no localized corrosion.

The high oxidation activity of permanganate was verified using a platinum electrode tested when permanganate was immediately added. Since platinum is thermodynamically unfavorable for corrosion, the determination of total current density obtained (37.6 $\mu A/cm^2$) can be attributed to permanganate oxidation reactions at the surface. Compared to C-276, a similar current density was obtained at similar conditions (42.3 $\mu A/cm^2$) confirming that for this alloy the total current density obtained immediately after addition was due to permanganate oxidation reactions. Pre-filmed C-276 in a formate-based solution also showed a high current density although there were no significant visual changes on the film after testing.

CPP results showed the appearance of a passive region when the test was performed long after permanganate was added. The results of the CPP for platinum, comparable to C-276, provides additional confirmation that that activity recorded was due to the electrochemical activity of permanganate oxidation. After removing the film (for the case of pre-filmed coupons) or layer from all the coupons used for electrochemical testing, no corrosion attack was observed. The absence of any type of corrosion attack after polarization to high potentials indicate that the material is not susceptible to localized corrosion when exposed to all the simulants used. In addition, OCPs measured during CPP experiments were highly positive at over 400 mV above the standard potential for hydrogen evolution reaction.

The mass loss corrosion rates for A537 carbon steel flat coupon and stressed samples was 0.18 mpy and 0.08 mpy on average, respectively, after coupon immersion for four weeks with no indications of localized corrosion, such as pitting and SCC. The corrosion rates obtained conforms with DWPF and Tank Farm norms of less than 1 mpy. A multicolored layer was observed on all the immersed coupons due to the permanganate oxidation exposure and was easily removed by immersing the coupons in 1 M HCl solution. Since corrosion was not observed, an assessment of the protective effects of the layer cannot be made. However, this layer does not seem to impact material performance and continual removal may not be necessary.

7.0 References

[1] D.P. Lambert, M.E. Stone, J.D. Newell, D.R. Best, and J.R. Zamecnik, “Glycolic-Nitric Acid Flowsheet Demonstration of the DWPF Chemical Process Cell with Sludge and Supernate Simulants”, SRNL-STI-2012-00018, Revision 1, August 2012.

[2] D.P. Lambert, M.E. Stone, J.D. Newell, D.R. Best, and J.R. Zamecnik, “FY13 Glycolic-Nitric Acid Flowsheet Demonstrations of the DWPF Chemical Process Cell with Simulants” SRNL-STI-2013-00343, Revision 0, March 2014.
[3] J.I. Mickalonis, K.J. Imrich, C.M. Jantzen, T.H. Murphy and J.E. Wilderman, “Corrosion Impact of Alternate Reductant on DWPF and Downstream Facilities,” SRNL-STI-2014-00281, Revision 0, December 2014.
[4] J.I. Mickalonis, “Impact of Glycolate Anion on AqueousCorrosion in DWPF and Downstream Facilities”, SRNL-STI-2015-00482, Revision 3, January 2019.
[5] C.J. Martino, J.M. Pareizs, and J.D. Newell, "Thermolytic Hydrogen Generation Testing of Tank 22 Material," Savannah River National Laboratory, SRNL-STI-2018-00385, Revision 0, 2018.
[6] J.R. Zamecnik, D.P. Lambert, W.T. Riley, and W.G. Ramsey, "Permanganate Oxidation of Defense Waste Processing Facility (DWPF) Recycle Collection Tank (RCT) Simulants – Protocol Runs for Nominal and Chemical Process Cell (CPC) Foamover Conditions," Savannah River National Laboratory, Aiken, SC, SRNL-STI-2019-000292, Revision 0, 2019.
[7] G. Chen and M. Clark, "Evaluation of Chemical Additives for Glycolate Mitigation," Savannah River Remediation, LLC, Aiken, SC, X-TTR-S-00068, Rev. 0, 2018.
[8] D.P. Lambert, “Task Technical and Quality Assurance Plan for Evaluation of Chemical Additives for Glycolate Mitigation,” Savannah River National Laboratory, Aiken, SC, SRNL-RP-2018-00358, Revision 0, 2018.
[9] C. F. Jenkins, “PERFORMANCE OF EVAPORATORS IN HIGH LEVEL RADIOACTIVE CHEMICAL WASTE SERVICE (U), Westinghouse Savannah River Company, Aiken, SC, WSRC-TR-97-00297, December 1997
[10] W. L. Daugherty, “Evaluation of Potential for Materials Degradation of DWPF Safety Class and Safety Significant Components (U), WSRC-TR-95-0385, Revision 0, Westinghouse Savannah River Company, 1995.
[11] R. B. Wyrwas, “Annual Report, Spring 2015: Alternative Chemical Cleaning Methods for High Level Waste Tanks – Corrosion Test Results”, SRNL-STI-2015-00302, Revision 0, Savannah River National Laboratory, Revision 0, May 2015.
[12] R. B. Wyrwas, “ANNUAL REPORT, FALL 2016: ALTERNATIVE CHEMICAL CLEANING OF RADIOACTIVE HIGH LEVEL WASTE TANKS- CORROSION TEST RESULTS”, SRNL-STI-2016-00465, Revision 0, Savannah River National Laboratory, September 2016.
[13] R.H. Ferguson, W.M. Lerch and J.E. Day, “Permanganate Decomposition in Alkaline Media”, Journal of American Chemical Society, 53, 126-137, 1931.
[14] R.E. Fuentes, “Run Plan for Corrosion Testing of Materials of Construction (MoC) of the Recycle Collectionof Tank (RCT) and Downstream Components After Glycolate Oxidation with Permanganate”, SRNL-L5400-2019-00004, Revision 0, June 2019.
[15] ASTM G30-97, “Standard Practice for Making and Using U-Bend Stress-Corrosion Test Specimens”, ASTM International, West Conshohocken, PA, 2016
[16] M. Siegfried, W. Ramsey and M. Williams, “Permanganate Oxidation of Defense Waste Processing Facility (DWPF) Recycle Collection Tank (RCT) Simulants Larger Scale Protocol Runs - Chemical Process Cell (CPC) Nominal and Foamover Conditions”, SRNL-STI-2019-00588, Revision 0, October 2019.
[17] ASTM G59 - 97, “Standard Test Method for Conducting Potentiodynamic Polarization Resistance Measurements”, ASTM International, West Conshohocken, PA, 2014.
[18] ASTM G61 – 86, “Conducting Cyclic Potentiodynamic Polarization Measurements for Localized Corrosion Susceptibility of Iron-, Nickel-, or Cobalt-Based Alloys”, ASTM International, West Conshohocken, PA, 2014.
[19] ASTM G31 – 12a, “Standard Guide for Laboratory Immersion Corrosion Testing of Metals”, ASTM International, West Conshohocken, PA 2013.

[20] B. Endrodi, S. Sandin, V. Smulders, N. Simic, M. Widlock, G. Mul, B.T. Mei and A. Cornell, “Towards sustainable chlorate production: The effect of permanganate addition on current efficiency”, Journal of Cleaner Production, 183, 529-537, 2018.

Appendix A. Electrochemical Test Details

Electrochemical corrosion methods were able to be used for the determination of susceptibility towards localized corrosion for most alloys tested more than three hours after permanganate addition. In addition, instantaneous general corrosion rates were able to be calculated at these conditions for A537 and 304L. Since permanganate oxidation can provide a current density that may overshadow the corrosion current density from metal dissolution when tested immediately, it may be not possible to calculate a corrosion rate for alloys tested at this particular instance. Electrochemical test details are provided in this appendix by considering the permanganate oxidation activity for instantaneous corrosion rates calculation and localized corrosion susceptibility determination from LPR and CPP, respectively.

OCP was measured until the potential of the sample equilibrated in solution and varied from two to three hours. An example of an OCP experiment is shown in Figure A-1 for a Hastelloy® C-276 freshly ground surface at 25 °C in the RCT simulant with maximum permanganate, as an example. The OCP started at negative potentials and was beginning to reach a plateau indicating potential stabilization. This OCP monitoring was performed before adding any permanganate, so starting potentials were negative. After the OCP was equilibrated to at least +/- 5 mV/min, LPR was performed over a potential range of +/- 30 mV around the OCP at a rate of 0.167 mV/s. Figure A-2 shows a voltage vs. current density plot obtained from an LPR experiment for this example. From the plot, the slope of the curve is used as the sum of the polarization resistance and solution resistance ($R_p + R_s$). Since the solution resistances were very low (i.e., the solution conductivity was high), R_s was considered negligible. To obtain the current density through electrochemical experiments ASTM G102[1] was used. The total current density i_{total} is calculated by using Faraday's Law as shown below,

$$i_{total} = \frac{B}{R_p} \quad (1)$$

where B is the Stern-Geary constant which is related to the electrochemical behavior at the surface of the alloy in the environment. The Stern-Geary constant is calculated from Tafel slopes from distinct linear regions near the OCP on a Potential vs. Log current density plot,

$$B = \frac{\beta_a \beta_c}{2.303(\beta_a + \beta_c)} \quad (2)$$

where β_a and β_c are the slope of the anodic and cathodic Tafel regions, respectively. To obtain the solution resistance and the anodic and cathodic Tafel reactions, a Tafel Plot or the initial part of a CPP scan can be used. For the calculations in this report, it was adopted the standard convention of 0.120 mV/decade as our anodic and cathodic slopes. This assumption was used to simplify the calculation of the current densities, assuming the same reaction mechanism was occurring (i.e., permanganate oxidation at the surface). When i_{total} is similar to the corrosion current density i_{corr}, corrosion rates can be calculated using the following expression,

$$CR = K \frac{i_{corr}}{\rho \, SA} EW \quad (3)$$

where K is a constant with value depending of units used, B is the Stern-Geary constant which is related to the electrochemical behavior of the material in the environment; EW is the equivalent weight (g) of the material; ρ is the material density (g/cm^3) and SA is the surface area of the sample (cm^2). To have the CR in mpy, K used was 0.1288.

Table A-1 lists the material densities and equivalent weights used in this work.

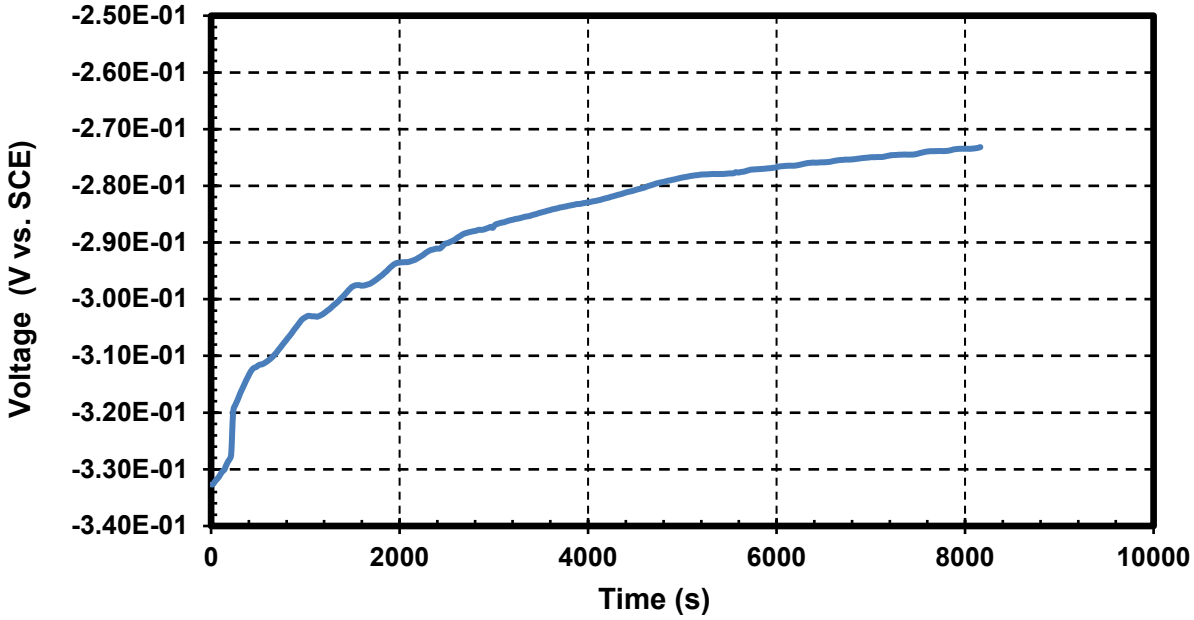

Figure A-1. OCP monitoring of Hastelloy® C-276 freshly ground surface at 25 °C immersed in RCT simulant with maximum permanganate.

Table A-1. Metal or Alloy corresponding density and equivalent weight used to calculate . instantaneous corrosion rate

Metal or Alloy	ρ (g/cm^3)	EW
A537 carbon steel	7.80	27.92
304L stainless steel	8.03	25.12

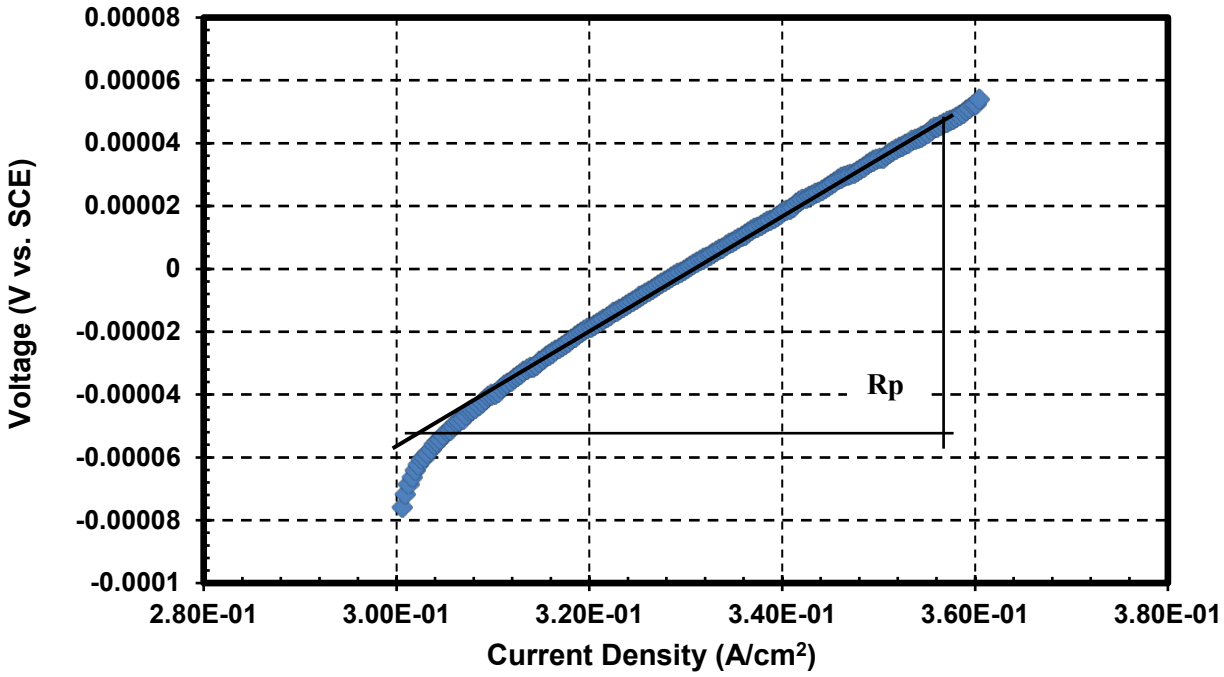

Figure A-2. LPR plot of Hastelloy® C-276 freshly ground surface at 25 °C immersed in RCT simulant with maximum permanganate.

After performing the LPR, the OCP was again recorded for 10 minutes to wait until the potential stabilized again and then a CPP experiment was performed. The CPP test is based on ASTM G61[2] and it was conducted by applying a cyclic potential ramp from -250 mV vs. OCP up to a potential of 2 V vs. SCE or a threshold current of 1 mA/cm^2 at a scan rate of 0.167 mV/s. The potential was scanned back to the OCP to complete the test. CPP assesses the susceptibility of the sample to localized corrosion by a comparison of the current densities of the forward and reverse scans. In some cases, especially after immediate addition of permanganate since permanganate oxidation is at the most active, CPP was unable to determine any localized corrosion susceptibility and conformed more into activity towards permanganate and promoting the growth of a layer on the surface.

To explain the CPP experiment and the information that can be obtained, important aspects of this approach are summarized here since they were utilized in the discussion of the results. Figure A-3 displays a schematic of an idealized CPP curve along with experimental parameters that are obtained from the curve. The curve presented has a positive closed loop hysteresis.

Definitions for these parameters:

- OCP is the open circuit potential. It is the potential at zero current, measured on the forward scan.
- E_{trans} is the transpassive potential and the increase in current for this case may be the result of other anodic reactions occurring (e.g., oxygen evolution).
- E_{CO} is the cross-over potential. It is the potential in the reverse scan at which the current density reduction causes the potential to cross-over the forward scan.
- i_{pass} is the passive current density. As the potential increases, the current density is maintained at approximately the same value in the passive range.

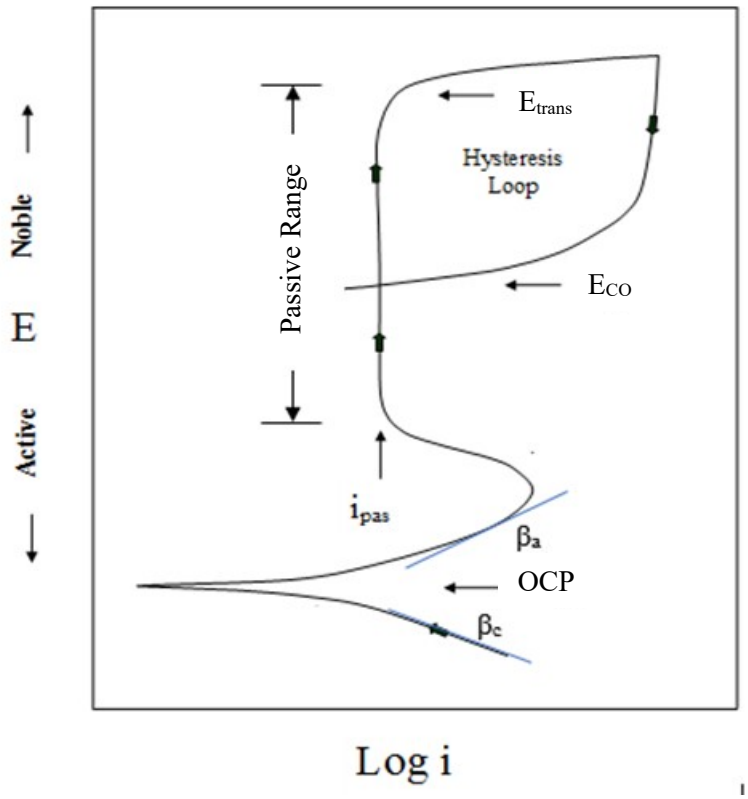

Figure A-3. Idealized CPP showing a positive closed loop indicating the passivation range and cross-over potential

At the start of the scan, the voltage sweeps until the current approaches to zero instantly and then continues until reaching the vertex current density or maximum potential. If there is a passive region, there is a current density that is nearly constant with little dependence of potential and that is known as the passive current density i_{pass}. At the reverse scan, the scan can go to a negative hysteresis or positive hysteresis. A negative hysteresis, where the current on the reverse is lower than during forward scan, may represent adherence and durability of the formed layer. On the contrary, a positive hysteresis, when the current on the reverse scan is higher than during forward scan, may be indicative of the increment in thickness or disintegration from surface of the formed layer.

References

1. ASTM G102 – 89, "Standard Practice for Calculation of Corrosion Rates and Related Information from Electrochemical Measurements," ASTM International, West Conshohocken, PA 2015.
2. ASTM G61 – 86, "Conducting Cyclic Potentiodynamic Polarization Measurements for Localized Corrosion Susceptibility of Iron-, Nickel-, or Cobalt-Based Alloys", ASTM International, West Conshohocken, PA, 2014.

Appendix B. Immersion Test Coupon Pictures

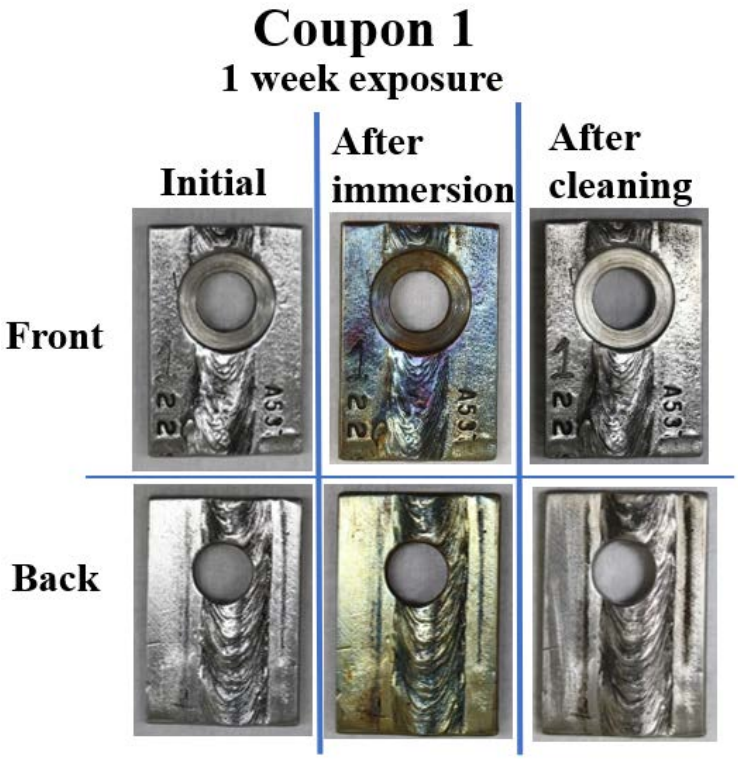

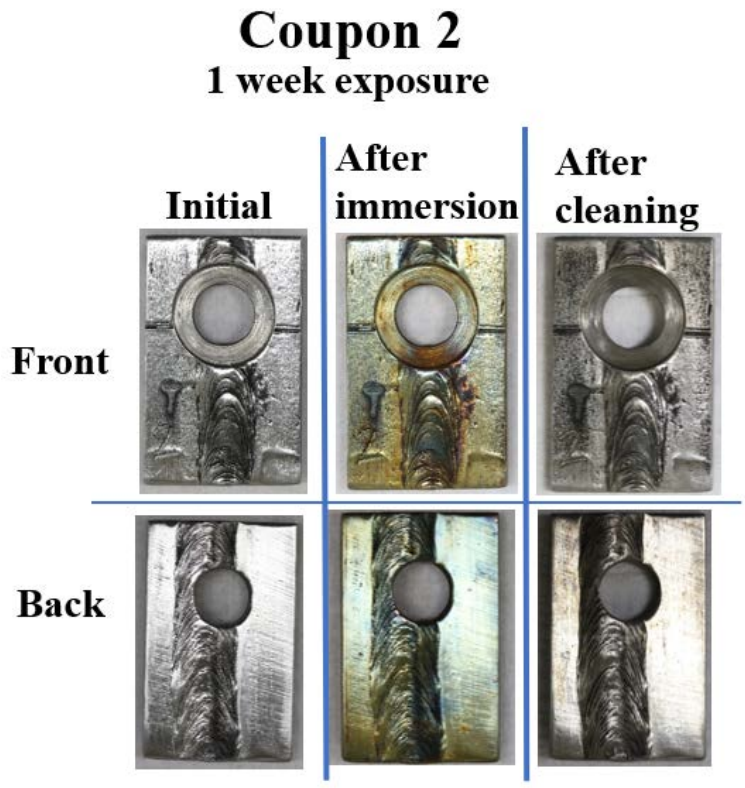

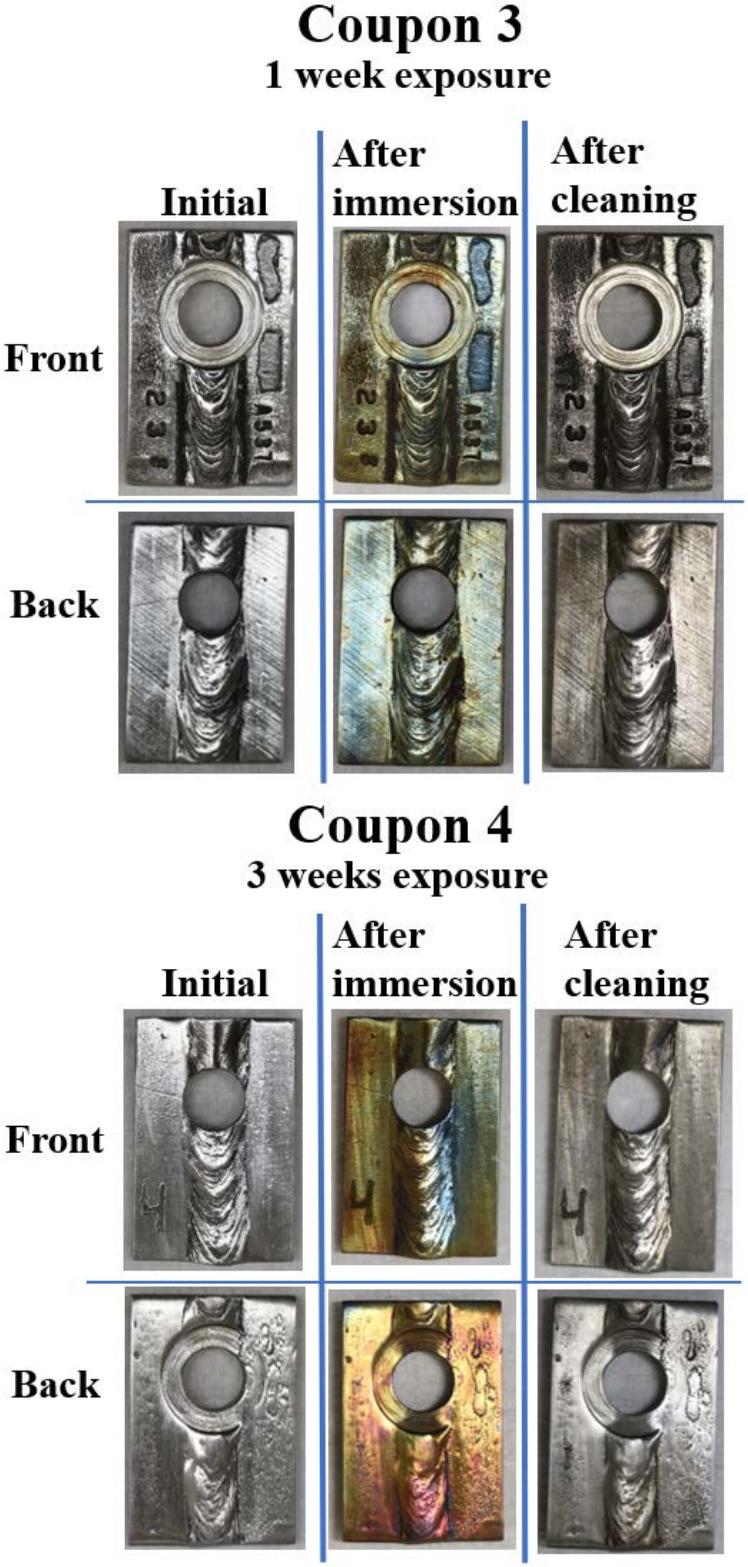
Coupon 3
1 week exposure
Initial
After immersion
After cleaning
Front
Back
Coupon 4
3 weeks exposure
Initial
After immersion
After cleaning
Front
Back

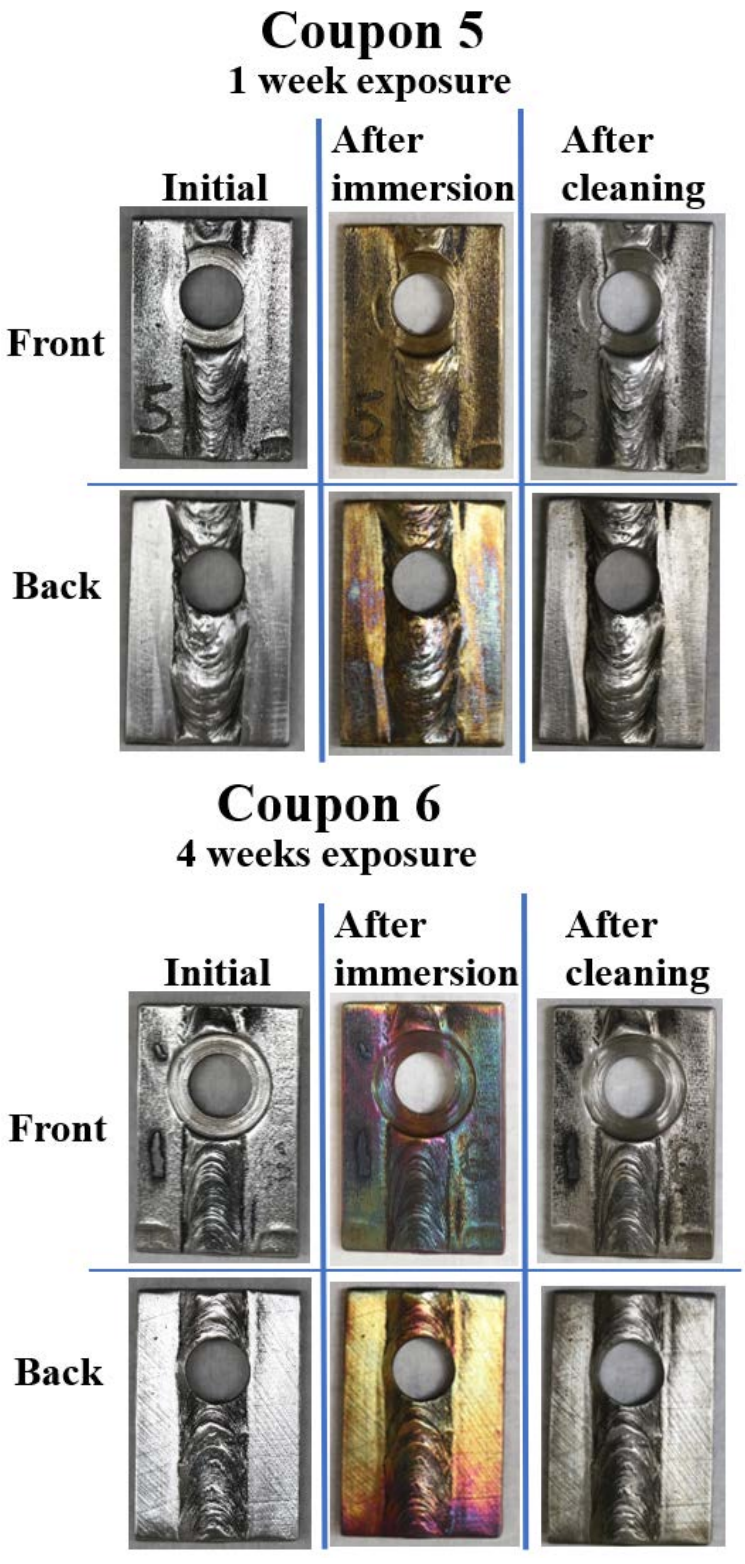
Coupon 5
1 week exposure
Initial
After immersion
After cleaning
Front
Back
Coupon 6
4 weeks exposure
Initial
After immersion
After cleaning
Front
Back

Coupon 228 – U-bend
4 weeks exposure

Initial

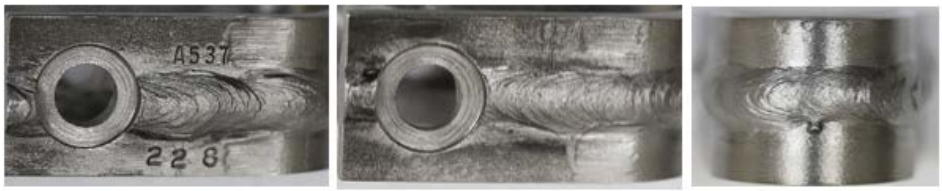

After immersion

After cleaning

Coupon 230 – U-bend
4 weeks exposure

Initial

After immersion

After cleaning

Distribution:

a.fellinger@srnl.doe.gov
aaron.staub@srs.gov
alex.cozzi@srnl.doe.gov
amy.ramsey@srnl.doe.gov
anthony.howe@srnl.doe.gov
arthur.wiggins@srs.gov
azadeh.samadi-dezfouli@srs.gov
barbara.hamm@srs.gov
bill.holtzscheiter@srs.gov
boyd.wiedenman@srnl.doe.gov
bruce.wiersma@srnl.doe.gov
celia.aponte@srs.gov
chris.martino@srnl.doe.gov
keisha.martin@srs.gov
christine.ridgeway@srs.gov
connie.herman@srnl.doe.gov
cory.trivelpiece@srnl.doe.gov
dan.lambert@srnl.doe.gov
daniel.mccabe@srnl.doe.gov
david.crowley@srnl.doe.gov
david.newell@srnl.doe.gov
earl.brass@srs.gov
eric.freed@srs.gov
erich.hansen@srnl.doe.gov
frank.pennebaker@srnl.doe.gov
grace.chen@srs.gov
gregg.morgan@srnl.doe.gov
hasmukh.shah@srs.gov
holly.hall@srnl.doe.gov
jack.zamecnik@srnl.doe.gov
james.folk@srs.gov
jeff.ray@srs.gov
jeffrey.crenshaw@srs.gov
jeffrey.gillam@srs.gov
john.iaukea@srs.gov
john.mayer@srnl.doe.gov
john.mickalonis@srnl.doe.gov
Joseph.Manna@srnl.doe.gov
kevin.brotherton@srs.gov
maria.rios-armstrong@srs.gov
mark-l.johnson@srs.gov
mason.clark@srs.gov
matthew.siegfried@srnl.doe.gov
matthew02.williams@srnl.doe.gov
michael.stone@srnl.doe.gov
nancy.halverson@srnl.doe.gov
patricia.suggs@srs.gov
paul.ryan@srs.gov
phillip.norris@srs.gov
Records Administration (EDWS)
richard.edwards@srs.gov
roberto.gonzalez@srs.gov
ryan.mcnew@srs.gov
samuel.fink@srnl.doe.gov
spencer.isom@srs.gov
stephanie.harrington@srs.gov
terri.fellinger@srs.gov
thomas.colleran@srs.gov
thomas.huff@srs.gov
timothy.baughman@srs.gov
todd.thompson@srs.gov
tony.polk@srs.gov
vijay.jain@srs.gov
william.pepper@srs.gov
william.ramsey@srnl.doe.gov